MIDDLE EAST TECHNICAL UNIVERSITY

DEPARTMENT OF ELECTRICAL and ELECTRONICS ENGINEERING

EE 463 – STATIC POWER CONVERSION I

Term Project Report

Eren Özkara 2232551

Büşra Nur Koçak 1929355

Yunus Çay 2166148

Table of Contents

1. Introduction

In this report, topologies that can be used in the project were discussed and compared. Then the simulation details and the details of the topology used were explained. Equations used in design, analytical calculations and design decisions were mentioned. The progress steps of the design were explained Then PCB design details were mentioned. Finally, the selected components and their properties were mentioned. Finally, bills of material list was made.

2. Topology Selection

In order to control the output current in the project, we need to use controlled rectifier or uncontrolled rectifier + buck converter topologies. Therefore, these topologies have been discussed.

2.1. Three Phase Thyristor

- Thyristor rectifier topologies are generally used in systems with high voltage and current.
- In this topology, the average output voltage of the thyristor rectifier can be controlled by adjusting the firing angle of the thyristors. Thus, output current can be adjusted with the firing angle.

$$V_{avg} = \frac{3\sqrt{2}}{\pi} V_{LL} \cos\alpha$$

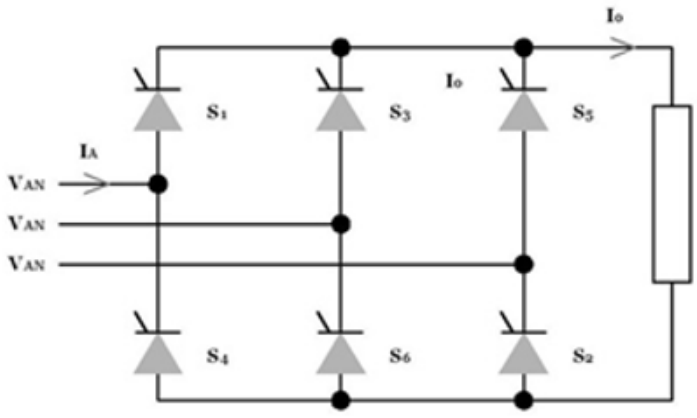

Figure 1 Three Phase Thyristor Topology and its Output Voltage Equation

Advantages

- This topology consists of only 6 thyristors; therefore, the topology structure is not complex.
- In this topology, the input current THD is low because the third harmonics of the input current are not observed.

Disadvantages

- Although this topology contains only 6 thyristors, thyristors are expensive components compared to diodes.
- To control six thyristors at the same time, six gate drivers and other components are required, which increases the cost considerably.
- Operating and controlling 6 gate drivers synchronously is a very complex process.

Three Phase Diode Rectifier with Buck Converter

- DC / DC converters are used in many areas such as electrical vehicles, PV - Grid systems.
- In this topology, AC voltage will be converted to DC with an uncontrolled rectifier and then to the desired DC voltage value with a buck converter.
- In this topology, the duty cycle of the buck converter is controlled by sensing the output current.

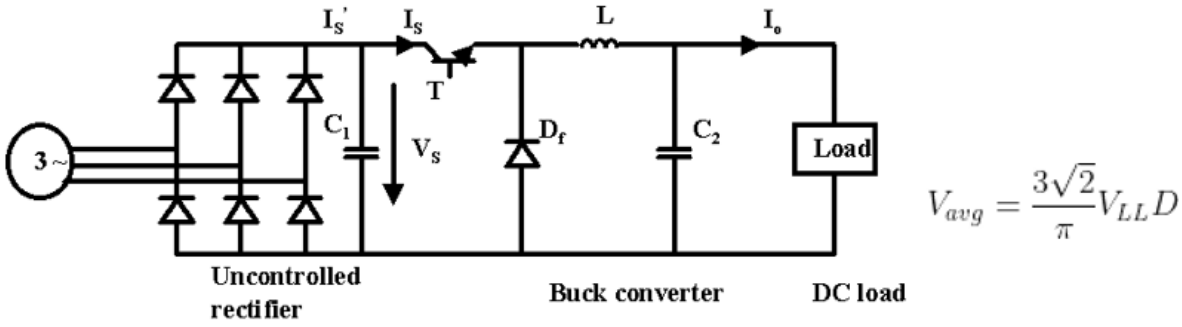

Figure 2 Three Phase Rectifier + Buck Converter Topology and its Output Voltage Equation

Advantages

- In this topology, the output voltage ripple can be easily reduced by placing a capacitor at the rectifier output and controlling the buck converter output voltage.
- This topology requires only one gate signal. This is a great advantage over controlled rectifiers. Also, the gate signal does not need to be synchronous.
- Although this topology requires more components, its cost is considerably lower than 3 phase-controlled rectifiers.
- In this topology, the input current THD is low because the third harmonics of the input current are not observed.

Disadvantages

- In this topology, its efficiency will theoretically be less since MOSFET and diode are used in addition to 3 phase-controlled rectifiers.
- Using an LC filter increases the size of the topology.

2.3 Modified Buck Converter

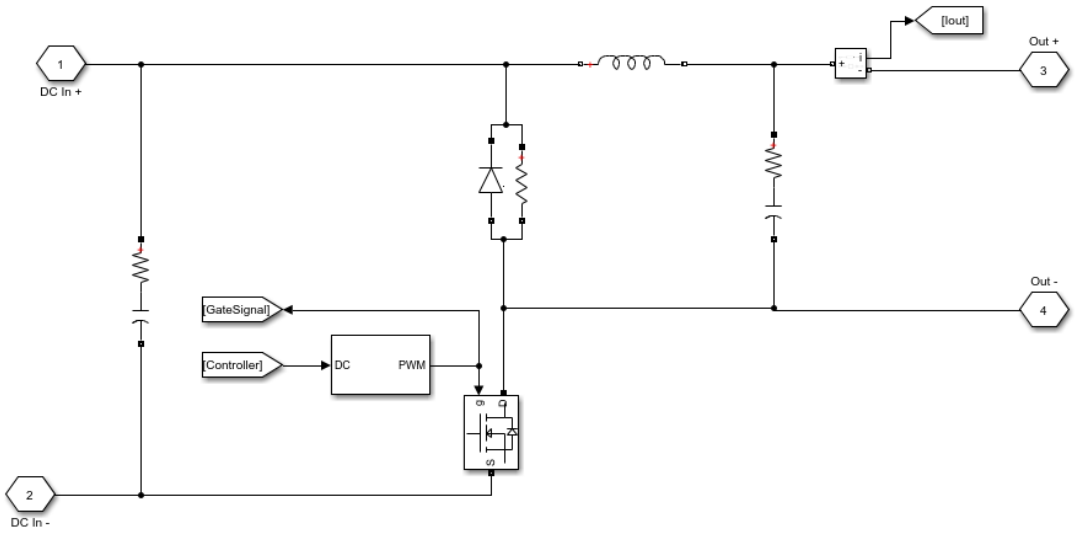

Figure 3 Modified Buck Converter Topology

Modified buck topology was discovered while researching about controllers for the project. A modified buck converter generally intends for high brightness LED applications. Also, these converters are designed as a constant current source to achieve the best lighting performance from the LEDs. In our project, constant output current is the main aim, therefore modified buck topology was chosen. Furthermore, modified buck topology is chosen for controllers of constant current applications because the power switch is connected to ground rather than the high side switch, like in a standard buck topology, thus control is easier. While the switch is on state, increasing current will flow through battery and when the switch is off state, the inductor keeps the current flowing in the same direction and the diode will be open and inductor current decreasing. This cycle continues like this. Details about relation between controller and modified buck converter will be explained in the controller part.

2.4 Final Topology the Project

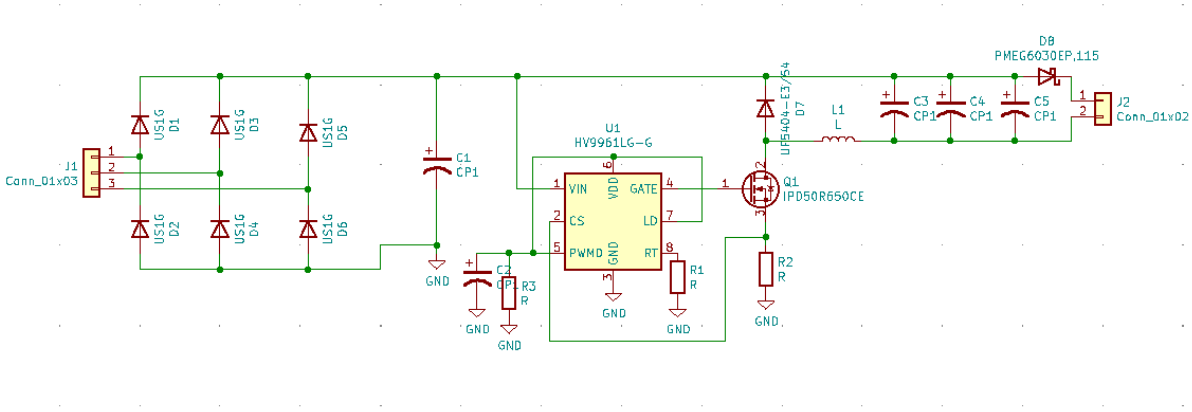

Figure 4 Final Topology of the Project

3-phase AC input voltage is converted to DC by using a 3-phase diode rectifier and DC link capacitor, then topology operate controller in constant current mode and obtain a constant output current with the buck converter. Before the battery, additional diode is used in topology. Thanks to the diode, when input voltage is lower than battery voltage, the battery will not lose energy and the topology will not be adversely loaded. Details of the topology will be explained later.

3. Detailed Simulation

3.1. Uncontrolled 3 Phase Rectifier

The modelled PMSM generator supplies three phase current to the system and 3-phase diode rectifier gives rectified signal as an output. The output voltage ripple is decreased with parallel capacitor which is place just before the buck converter. The modelled PMSM generator and rectifies can be seen in Figure 5. Input of generator is mechanical torque and other specifications of PMSM are provided in the project description.

The generated voltage difference on motor terminals depends on mechanical torque. Since the load current does not change, electrical torque of generator is constant, so difference between mechanical torque and electrical torque returns as a speed of shaft according to Equation (1). The constant electrical torque results in a significant observation about efficiency. Increase in the speed of rotor results in a more viscous friction loss. Hence, for constant output power applications are not efficient from the point of mechanical power and output power view.

$$T_e = T_f + B_m w + T_m \quad (1)$$

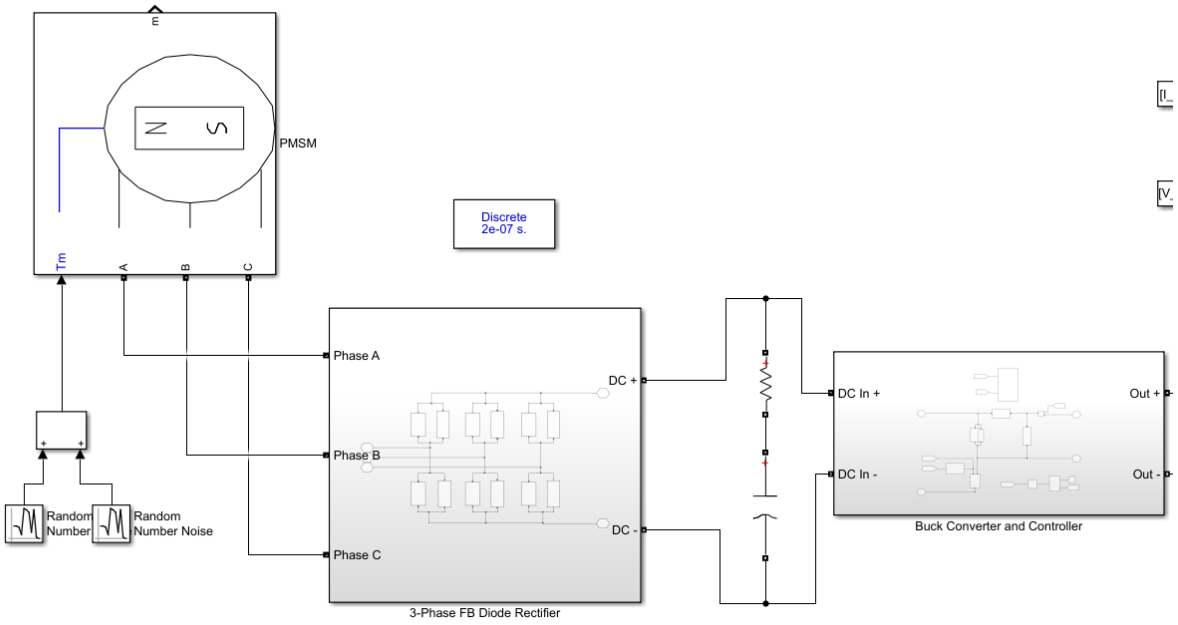

Figure 5 Modelled PMSM generator and 3-phase FB diode rectifier

3-phase diode rectifier works without a control which is handled by characteristics of diode. The output voltage equals to the greatest line-to-line instantly. Since, the ripple frequency is six times of input line-to-line voltages, ripple is considerably low. The mean voltage of output without a dc-link capacitor is calculated in Equation (2). However, the output voltage is slightly less than generated voltage in generator due to commutation and stator resistance. While generator current results in a voltage drop on stator resistance, the armature reactance causes commutation.

$$V_{mean} = \frac{3\sqrt{6}V_{s,RMS}}{\pi} \tag{2}$$

Output voltage ripple decreases as the pulse number of rectifiers increases. The 3-phase diode rectifier is called as 6-pulses rectifier. In addition to pulse number, DC-link capacitor filters out high frequency components of output voltage, so that the output voltage ripple decreases. Thus, the DC-link capacitor is placed just before the buck converter to decrease ripple as shown in Figure 5.

3.2. Buck Converter

General Structure and Calculations of Buck Converter

The DC voltage, which is the output of the three-phase full wave diode rectifier described in Part 3.1, have been connected into a buck converter to step down the voltage value from 250 V (Vmax) to 25 V nominal value for charging the battery. The main structure of the buck converter can be seen from the Figure 6. An approximate inductance and capacitance values have been calculated by specifying the on and off cases of switching element of the buck converter, which is MOSFET in this case.

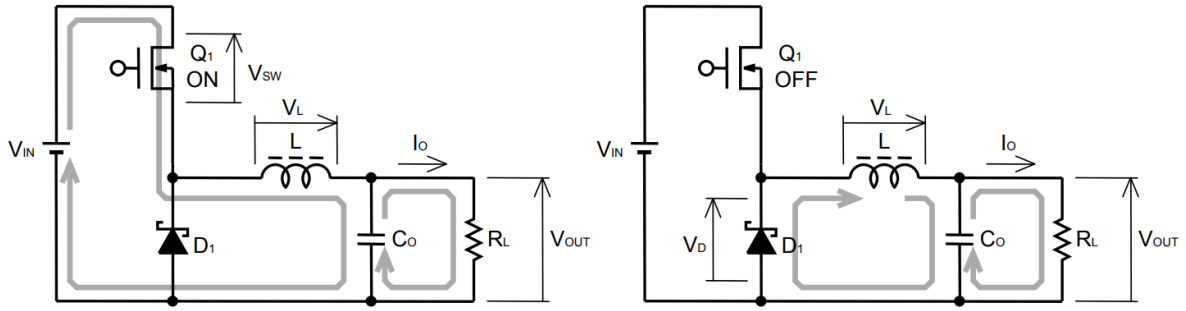

Figure 6 Buck converter ON and OFF cases of the MOSFET

The output current of the buck converter is intended to be 2A with %20 of average current as ripple, while the battery is being charged. Therefore, ON and OFF states of the MOSFET have been considered separately for the same output current level to specify a formula for calculating required inductance value to apply intended output current ripple, Equation (3).

$$L = \frac{(V_{IN} - V_{SW} - V_{OUT}) \times (V_D + V_{OUT})}{(V_{IN} - V_{SW} + V_D) \times f_{SW} \times r \times I_{OUT}} \quad (3)$$

V_{IN}: Input Voltage (V)

V_{SW}: MOSFET ON state voltage drop (V)

V_{OUT}: Output Voltage (V)

V_D: Diode forward voltage drop (V)

f_{SW}: Switching frequency (Hz)

r: Output current ripple ratio

I_{OUT}: MOSFET ON state voltage drop

The values specified above taken into consideration to calculate only an approximate inductance. According to these L have been calculated as 5.76 mH, which is known to be very high value for an inductor. The main reason for such high inductance is to decrease the ripple on the output current. Moreover, since the frequency value is located in the denominator as seen in the Equation (3) , the use of low frequency caused the inductor value to increase. Because, the ripple voltage already specified before, frequency is chose to be the factor that can be changed to adjust the inductance value. Considering the effects of the frequencies in the 10 kHz- 100 kHz range on the conduction losses and switching losses, 50 kHz have been seen as a suitable value to reduce the inductor value by keeping the overall power loss level sufficiently low. Therefore, the inductor value has been achieved to decrease to 1.2 mH, which is 5 times less than the value calculated before, by changing the switching frequency with 50 kHz.

The conduction losses and switching losses of switches are the most important parameters effecting efficiency of converter. Since the different step-down converter topologies are available, the switches are named as high-side and low side switch. While the high side switch represents the MOSFET, low-side switch represents the diode for non-synchronous buck converter. The calculation of conduction losses for different type of switches are shown in Table 1.

Table 1 is used to decide step-down converter topologies between synchronous and non- synchronous converters. The duty cycle is taken as 0.1 for the sake of simplicity according to given mechanical torque values. Therefore, conduction losses of low-side switch are dominant. On the other hand, IGBT is eliminated due to increase in switching frequency. Whereas MOSFETs are generally used for high frequency and relatively low reverse voltage applications, IGBTs are chosen for low frequency and high reverse voltage applications.

All in all, the high-side switch is MOSFET type and the low-side switch can be diode or MOSFET. Although the type of low-switch affects the topology, the consideration of cost and efficiency is more important than driver characteristic and topology. Hence, low-switch is chosen as diode, which makes the converter non-synchronous.

Table 1 Conduction loss of high-side and low-side switches

Switch	Type	Conduction Loss
High-side	MOSFET	$P_{cond,H} = D * I_{O,AVG}^2 * R_{DS,ON}$
High-side	IGBT	$P_{cond,H} = D * I_{O,AVG} * V_{CE}$
Low-side	MOSFET	$P_{cond,L} = (1-D) * I_{O,AVG}^2 * R_{DS,ON}$
Low-side	IGBT	$P_{cond,L} = (1-D) * I_{O,AVG} * V_{CE}$
Low-side	Diode	$P_{cond,L} = (1-D) * I_{O,AVG} * V_{FD}$

If switching loss of diode and MOSFET were high compared to conduction loss, the selection of switch type could depend on switching loss and switching frequency. However, the switching loss of components are approximately 5 times less for MOSFET and 3 times less for diode. The switching loss calculations can be seen in Table 2.

While gate driver current and gate charge are considered for MOSFET, reverse recovery charge is considered as an important parameter for selection. Thus, gate driver is chosen as strong to supply high gate currents and type of diode is selected as fast diode.

Table 2 Switching loss of high-side and low-side switches

Switch	Type	Switching Loss
High-side	MOSFET	$P_{SW,H} = V_{in} * I_O * f_{sw} * \frac{Q_g}{I_g}$
Low-side	Diode	$P_{SW,L} = f_{sw} * V_{in} * Q_{rr}$

While the inductor is effective in adjusting the output current ripple, capacitor plays an important role in output voltage ripple. Moreover, ESR of the capacitor which stands for 'Equivalent Series Resistance' is also an important factor while choosing a capacitor, as can be seen from the Equation (6), where ESL value is assumed to be 0 H. Both ON and OFF states of the MOSFET have been taken into consideration while analyzing the factors affecting the capacitor value.

$$\Delta V_{ORPL} = \Delta I_L \left(\frac{1}{8 \times C_O \times f_{SW}} + ESR\right) + ESL \frac{V_{IN(MAX)}}{L} [V_{P-P}] \quad (4)$$

$V_{IN(MAX)}$: Maximum Input Voltage (V)

ΔI_L: Inductor ripple current (A)

C_O: Output capacitor (F)

ESR: Equivalent series resistor of output capacitor (Ω)

ESL: Equivalent series inductor of output capacitor (H)

The finalized approximation used in the capacitor calculations can be seen from Equation (6).

$$C_o = \frac{\Delta I_L}{8 * f_{sw}} * \frac{1}{\Delta V_{ORPL} - \Delta I_L * ESR - ESL * \frac{V_{in(max)}}{L}} \quad (5)$$

$$C_o = \frac{1}{8 * f_{sw} * (\frac{\Delta V}{\Delta I_L} - ESR)} \quad (6)$$

Hence, approximate capacitor value is calculated as 50×10^{-6} with 0.2 Ω ESR value. Because one of the most important parameters are specified as the ESR in output voltage ripple and capacitor calculations, it was decided to pay attention to the small ESR value, during the selection of capacitor. As the output voltage and current ripples of the converter is already specified before, an upper limit has been determined for the ESR value.

Buck Converter Simulation with Estimated Values

An example circuit have been set, using the estimated values, which are calculated. The aim of this circuit is to show that the calculated inductor and capacitor values can reduce the input voltage level to the desired output voltage level with the specified ripple voltage. Moreover, inductor effect on output current waveform with the addition of a control system can be seen in Figure 8.

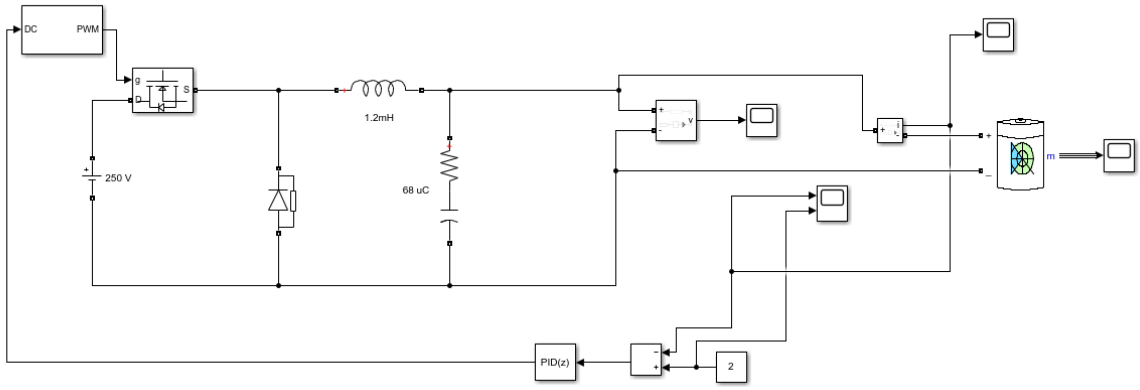

Figure 7 Buck converter Simulink circuit with PI controller

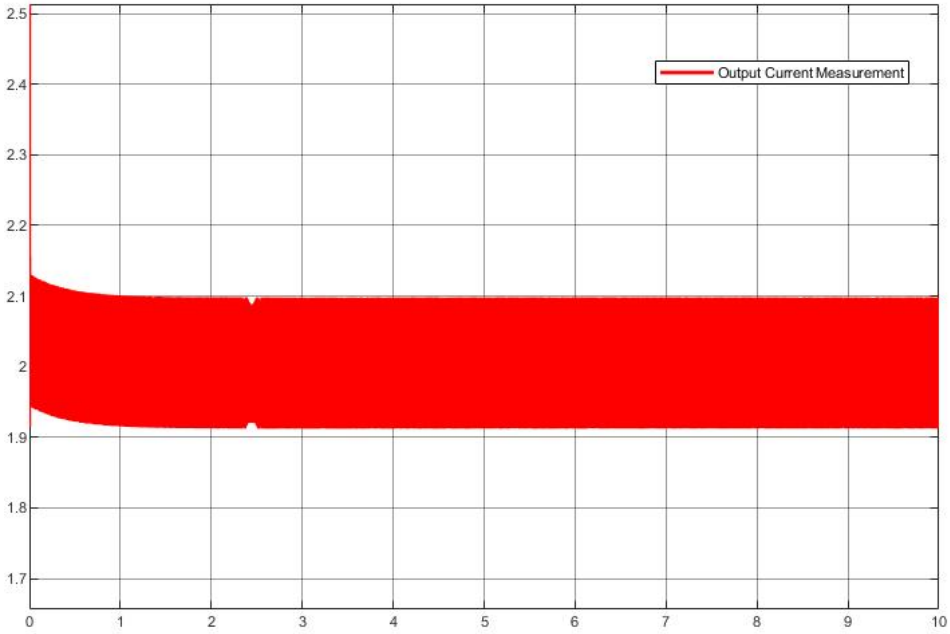

Figure 8 Output current measurement of the buck converter

3.3. Battery

In this part, battery part will be analyzed, and some test will be applied.

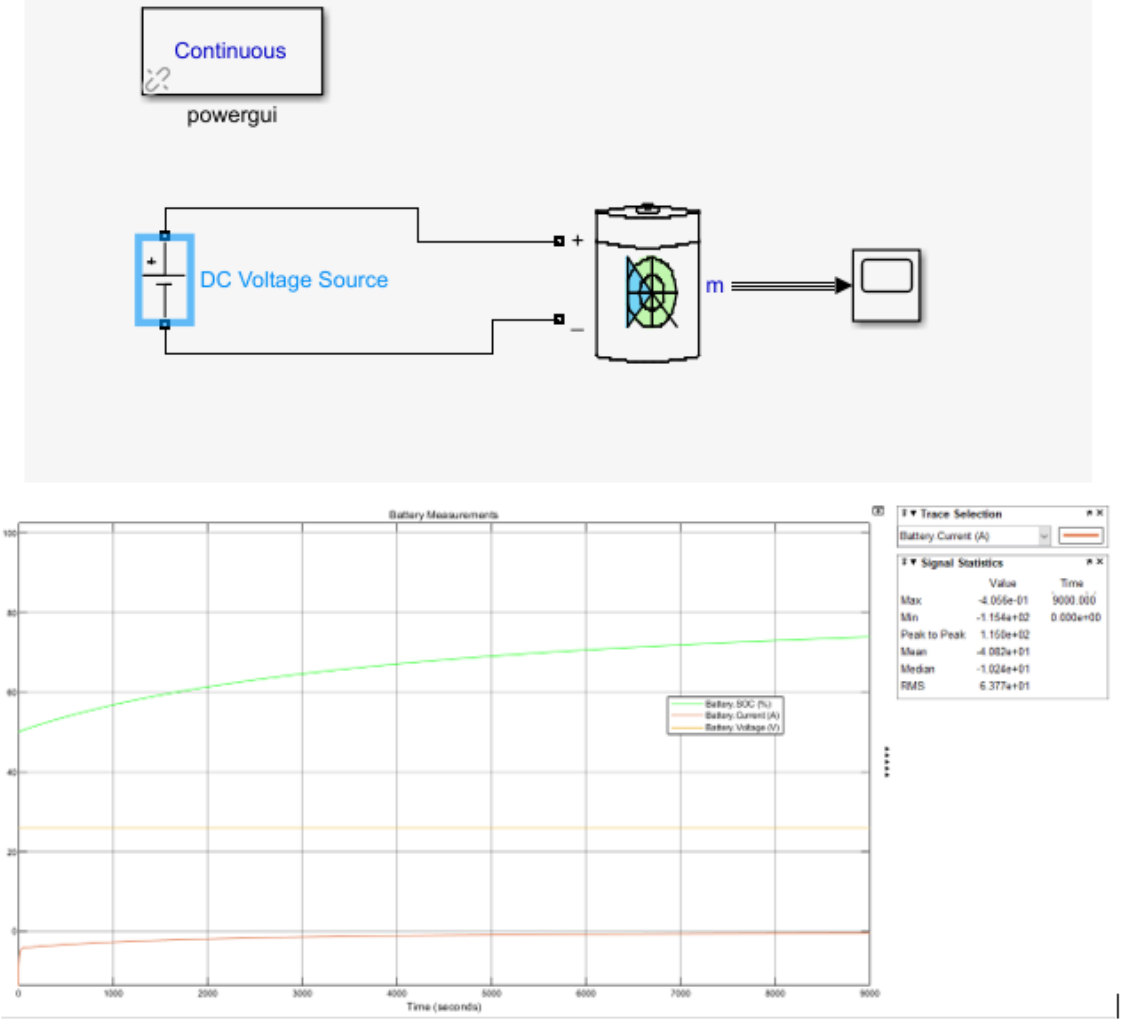

Figure 9 Constant Voltage Battery Test

In this test, battery behavior was observed when a constant voltage of 25 volts was applied to the battery. As can be seen from the graph, it is not enough to give constant input voltage to obtain constant current. Therefore, an increasing voltage must be applied to the battery.

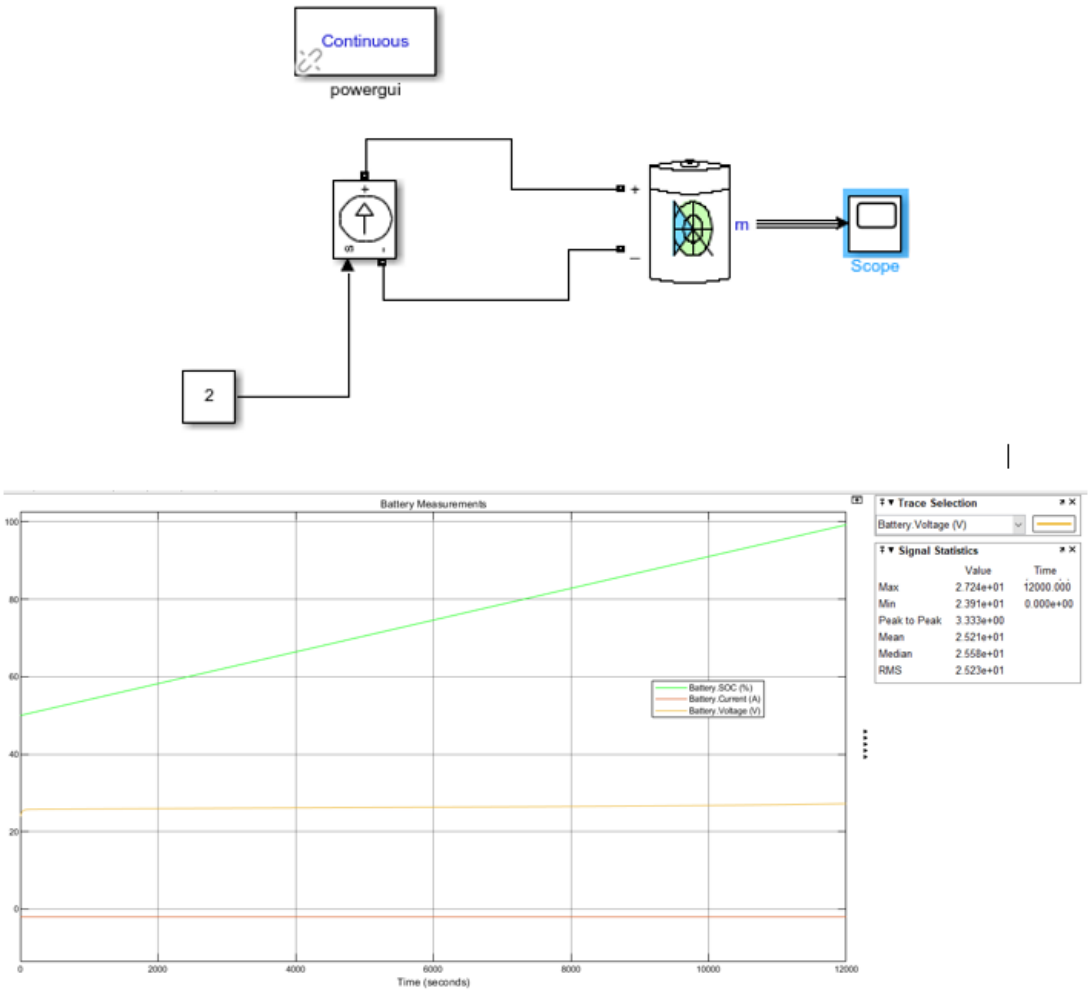

Figure 10 Constant Voltage Battery Test

In this test, a constant input current of 2 amps was applied to the battery. As can be seen from the graph, an increasing voltage between 24-27 volts should be applied to the battery to charge from %50 to %100.

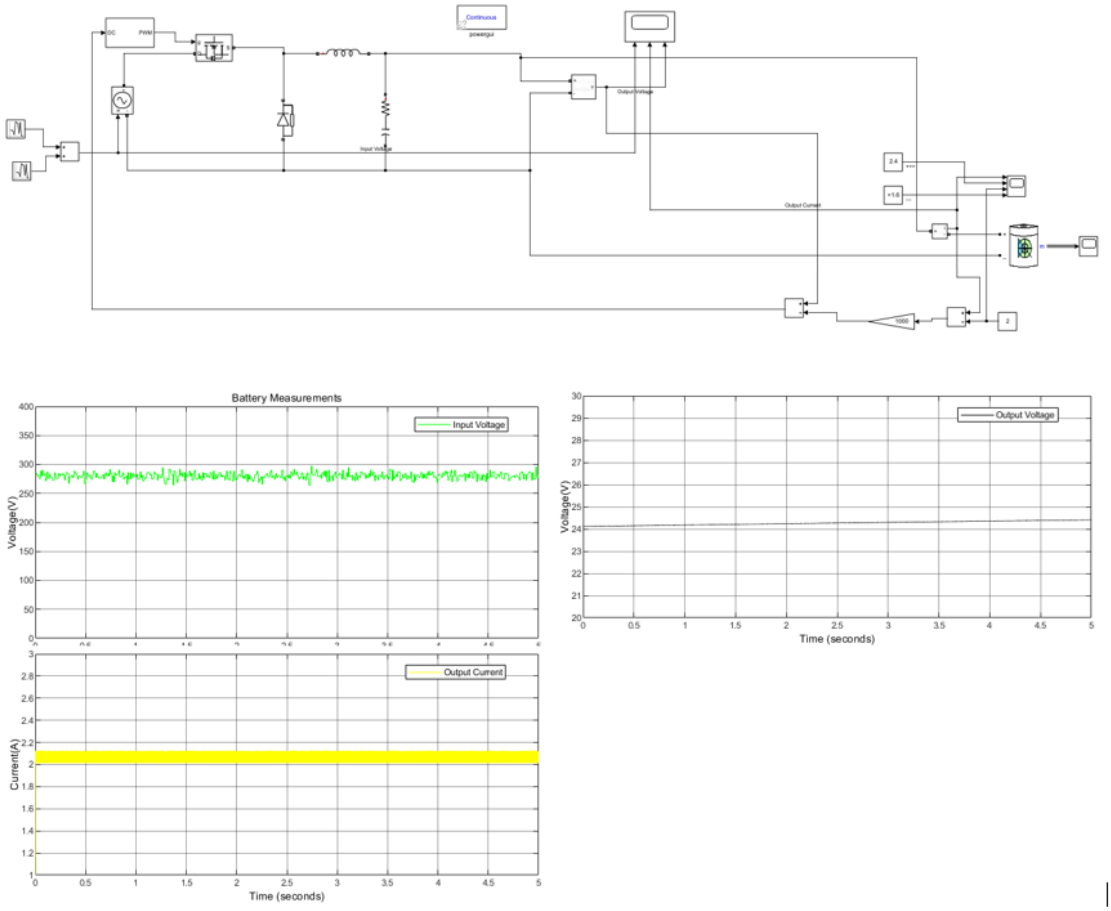

Figure 11 Buck Converter and Battery Test with P controller

In this test, the battery and buck converter part are connected. Buck converter's input is symbolized as noisy input with an average value of 280 V. In the test, an offset was observed in the output, so the P controls part will be converted into PI controls. Also, controller is simplified. In the following sections, all parts were combined with the rectifier and simulations were made in discrete time.

3.4. Controller

The control of battery current is the requirement defined as system requirement. The control topology has been defined in *Figure 12* in the simulation report. The sense current is processed, and the processed current information is provided to gate driver. The desired output current is 2A.

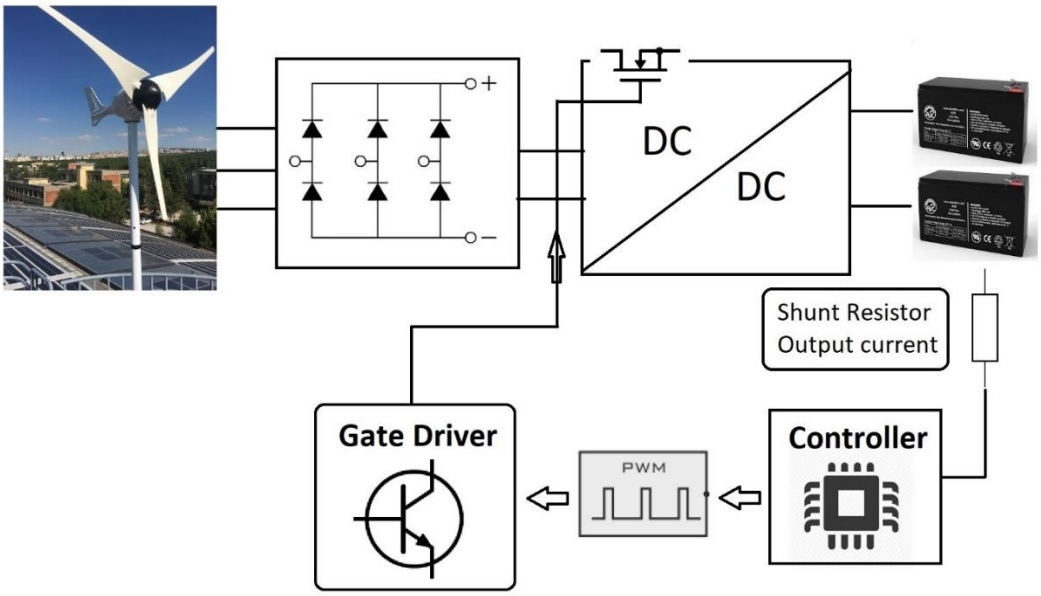

Figure 12 Block diagram of system and controller

The controller simulations are handled with PI controller block in Matlab/Simulink. The current ripple is satisfied with in limits defined by min current and max current lines as seen in Figure *13*. The frequency is selected as 50kHz for the simulation.

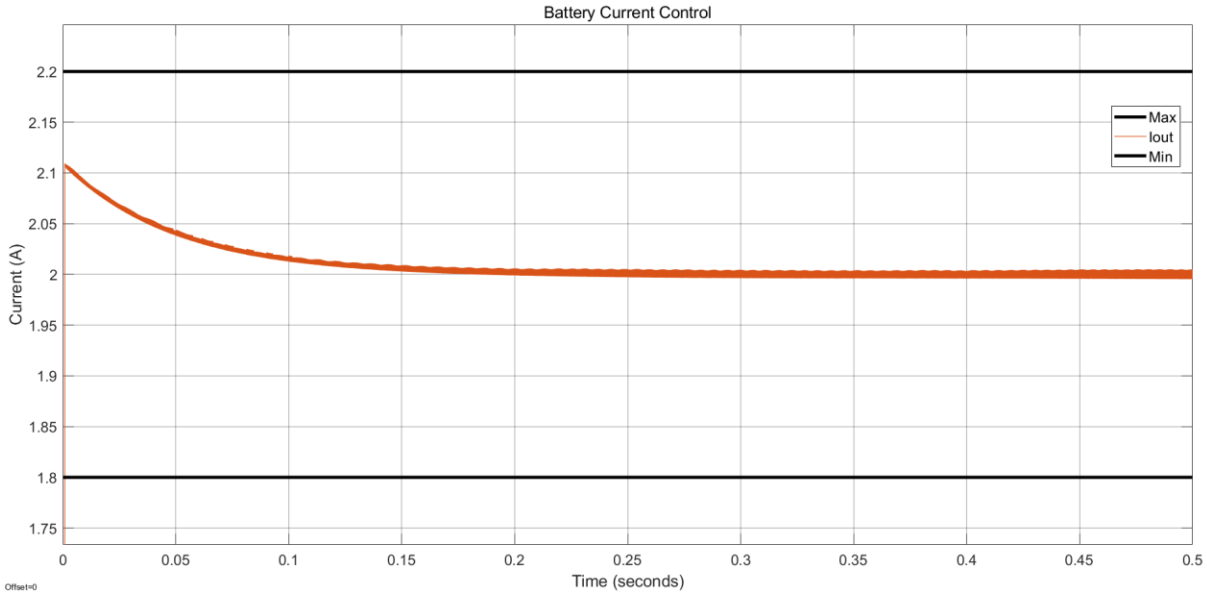

Figure 13 Battery current control with PI controller in Simulink

Controller selection is the one of time consuming part of the project. The vast majority of manufactured controllers have low voltage limits and digital controllers restricts the system to usage of isolation. Isolation is disadvantage due to high size and cost. On the other hand, low cost and size can be gained from internal gate driver controller. The desired controller is all in one. *Table 3* shows different type of manufactured controllers.

Table 3 Summary of different type of controllers

Type	Including	Limits
Switcher	- Switch - Controller - Gate driver	Low input voltage levels Low power applications
External regulator	- Controller - Gate driver	Low voltage levels
Digital controller	- Controller	Isolation

The controller research has expanded to find an all-in-one type of controller within voltage limits. As a result of research, led driver controllers have been found. The represented led driver, AL9910A, has replaced with led driver, HV9961 controller. The functional block diagram of AL9910A and HV9961 controllers can be seen in *Figure 14*.

Both led driver can control the current with sense resistor, linear dimming and PWM dimming. Since the current of battery is constant, the sense resistor is used. The controller directly connected to input voltage and linear voltage regulator is used to get constant voltage for internal components such as gate driver. Sensed output current is compared with reference. Then, the gate driver turns on and off the switch

according to comparison, which is hysteresis control. However, HV9961, have average current control logic inside. The comparison of the former and the latter led driver controller is shown in table 4.

Table 4 Comparison of Controllers

	AL9910A	HV9961
Input voltage range	- 20V - 520V	- 10V - 450V
Switching type	- Non-synchronous	- Non-synchronous
Control	- Current sense - Linear dimming - PWM dimming	- Current sense (Average control) - Linear dimming - PWM dimming
Switching frequency	- Constant f_{sw} - Constant T_{off}	- Constant T_{off}
Soft start	- External (Capacitor connection to LD pin)	- External (Capacitor connection to LD pin)
Price (1000 pieces)	- 0.84$	- 1.15$

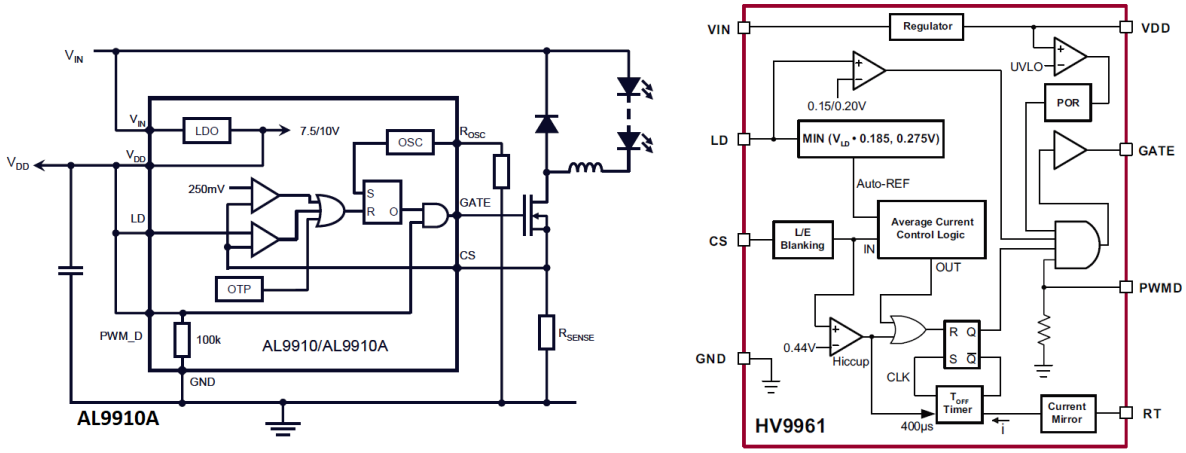

Figure 14 Functional block diagrams of led driver controllers, AL9910A and HV9961

The HV9961 controller have average current control logic to decrease current ripple. The switching frequency of the controller changes due to characteristic of the controller. The constant off-time determination provides the converter with constant current ripple if inductance is sufficiently high, since output voltage and inductance value don't change. The on-time changes according to input voltage. As the input voltage increases, on-time decreases so that frequency increases. Hence, the maximum limits of input voltage and current ripple determines maximum switching frequency as seen in Equation xxx.

$$\Delta I_L = \frac{V_{out}(1-D)T_s}{L} = \frac{V_{out}\,T_{off}}{L}$$
$$\frac{T_{on}}{T_s} = D = \frac{V_{out}}{V_{in}} \quad (7)$$

The off-time is adjusted from the R_T pin of HV9961 controller according to Equation xxx.

$$T_{off}(\mu sec) = \frac{R_T(k\Omega)}{25} + 0.3, 30k\Omega \leq R_T \leq 1M\Omega \quad (8)$$

HV9961 controller does not have soft starter. However, the characteristic of linear dimming provides the circuit with soft start by external capacitor. Figure xxx shows the typical application circuit of HV9961. The capacitor connected to VDD, PWMD and LD pins of controller starts to charge up to VDD voltage initially. When the voltage on capacitor is lower than 1.5V, the linear dimming dominates the current reference voltage so that soft start applies.

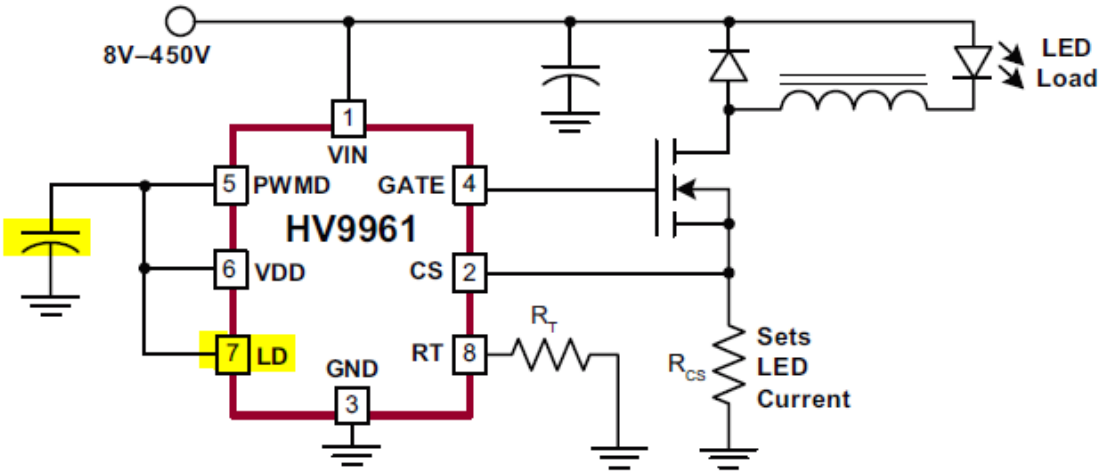

Figure 15 Sample Topology of HV9961

The HV9961 provides the system with low cost and small size. Also, because the switching frequency decreases as input voltage decreases, the switching losses decreases while the current ripple stays constant. On the other hand, the LDO decreases the efficiency of controller and the reference voltage of controller may result in a high resistive loss on shunt resistor as output current increases.

4. Loss Calculations

The practical loss mechanisms are modelled and calculated according to datasheets of the components. The losses can be classified as switching losses and conduction losses. The losses of buck converter are shown in Table xxx.

The formal, AL9910A, controller have constant switching frequency and conduction losses that changes in parallel with the input voltage. On the other hand, the latter, HV9961, controller adjust the switching frequency according to the input voltage, so that switching loss depends on input voltage.

Table 5 Power Loss Equations

Loss mechanism	Component	Model
Conduction	MOSFET	$P_{on,M} = \left[I_{out}^2 + \frac{\Delta I_L^2}{12}\right] R_{on,M}\, D$
Switching	MOSFET	$P_{sw,M} = \frac{1}{2} V_{in} I_{out} (t_{rise} + t_{fall}) f_{sw}$
Switching – Output capacitance	MOSFET	$P_{coss} = \frac{1}{2} V_{in}^2 (C_{DS} + C_{GD}) f_{sw}$ $P_{coss} = E_{coss}\, f_{sw}$
Switching – Gate charge	MOSFET	$P_G = Q_g\, V_{gs}\, f_{sw}$
Conduction	Diode	$P_{on,D} = V_f I_{out} (1 - D)$
Switching – Reverse recovery	Diode	$P_{sw,D} = \frac{1}{2} V_{in}\, I_{rr}\, t_{rr}\, f_{sw}$
Conduction – Copper loss	Inductor	$P_L = \left[I_{out}^2 + \frac{\Delta I_L^2}{12}\right] R_L$
Conduction	Shunt resistor	$P_{shunt} = \left[I_{out}^2 + \frac{\Delta I_L^2}{12}\right] R_{shunt}$

The contributions from different kind of loss mechanisms and total power loss of MOSFET and diode are given in *Figure 16* and *Figure 17*, respectively.

The conduction losses and switching losses of MOSFET are dominant at low input voltages and high input voltages, respectively, which results from the change of frequency, reverse voltage, and duty cycle. On the other hand, conduction losses of MOSFET are dominant at both low input voltages and high input voltage due to high forward voltage of diode.

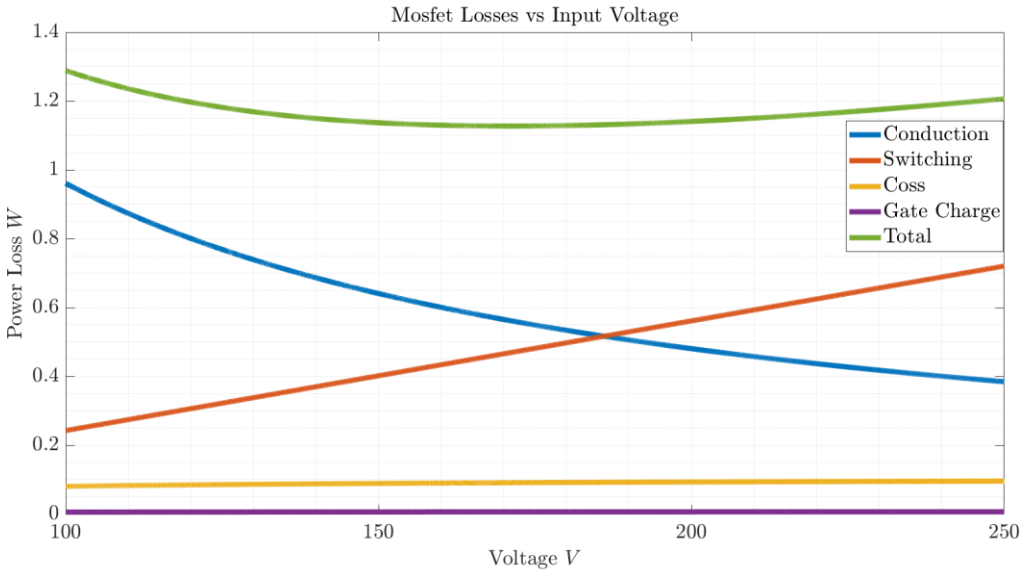

Figure 16 Conduction, switching and total power losses of MOSFET

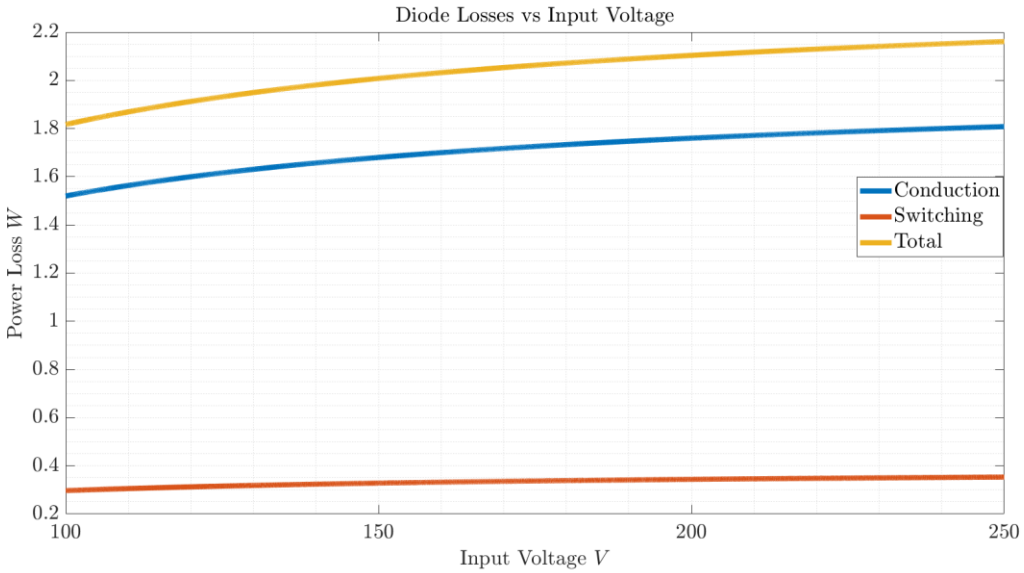

Figure 17 Conduction, switching and total power losses of Diode

There are other loss mechanisms due to resistive losses of inductor and shunt resistor. Since the output current pass through the inductor and shunt resistor, magnitude of the resistive losses depends on the output current. The power loss calculations for resistive losses are shown in *Table 6*.

Table 6 Resistive losses of inductor and shunt resistance

Component	Power Loss
Inductor	1.485W
Shunt resistor	0.548W

5. Thermal Calculations

The thermal calculations are hand calculations. The consideration for the thermal management is based on that each component generating heat is assumed as surrounded by air. The used thermal resistances are junction-to-case and case-to-ambient resistance to reveal whether heat-sink is needed or not.

The thermal calculation is processed iteratively. The junction temperature and on resistance of MOSFET have direct relation. Hence, the resistance should be increased iteratively up to where founded junction temperature and assumed junction temperature are equal. The iterative steps for thermal calculation of MOSFET is shown in *Table 7*. The junction-to-ambient thermal resistance is assumed 60°C/W.

Table 7 Iterative thermal calculations for MOSFET

$R_{thJA,TYP}$ - $R_{thJA,MAX}$: 35°C/W - 62°C/W			
R_{DS}	**Assumed T_J - T_A**	**Max. Power Loss**	**Calculated T_J**
0.60Ω	25°C - 25°C	1.05W	88°C
0.95Ω	88°C - 25°C	1.24W	99.4°C
1.05Ω	99.4°C - 25°C	1.32W	104.2°C
1.10Ω	104.2°C - 25°C	1.38W	107°C
1.12Ω	107°C - 25°C	1.40W	109°C

The found maximum junction temperature of mosfet is calculated as 110°C. This value is calculated with maximum ratings of thermal resistance and power. The maximum junction temperature is 150°C. Hence, the safety region can be increased more for the sake of compensation of increase in ambient temperature. The safety region is increased with usage of PCB as a heatsink. Even if the copper can be the best thermal conductor, the thermal resistance of the PCB is not good much. The simulation from one of the webside can be seen in *Figure 18*. The thermal resistance of PCB is as high as the junction-to-ambient thermal resistance of mosfet. Although effects of the thermal vias on PCB is not considered, the junction temperature is high. However, aim to get minumum size and cost restricts the circuit from heatsink. The thermal vias holes are placed close to the mosfet and leads of the diode. Also, placing thermal vias can be considerably effective due to the two layer PCB.

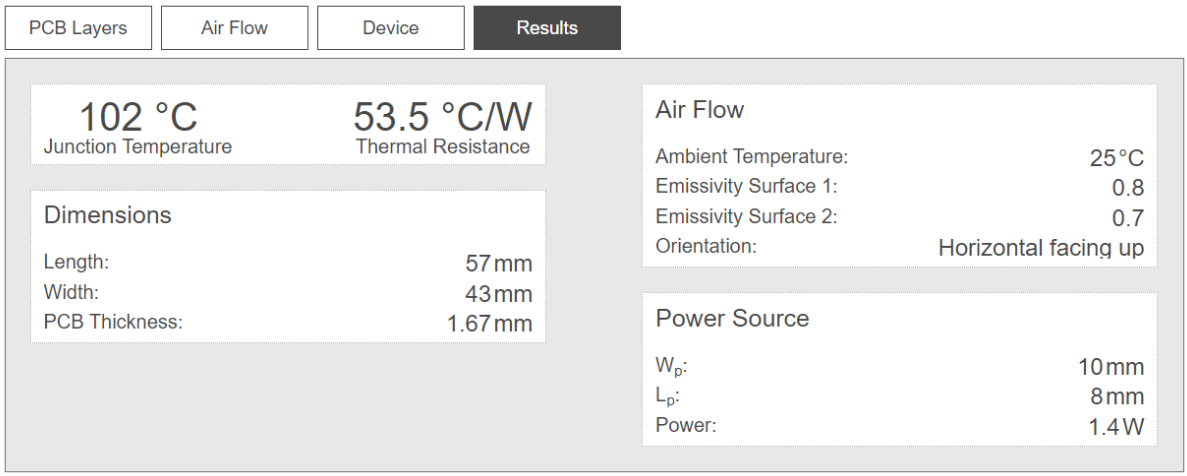

Figure 18 PCB thermal simulation

The thermal calculations for the diode is given in Table 8. The selected diode is type of through hole, so that the diode dissipates heat power from leads and case. The connection between diode and PCB is relatively small and thermal resistance of PCB is not as low as the thermal resistance of junction to ambient. Therefore, thermal calculation is calculated with consideration of heat transfer between case and air and the heat transfer between PCB and leads can be considered as safety margin.

Table 8 Diode Thermal Calculations

Forward Voltage - V_F	Max. Power Loss	R_{thJA}	Calculated Max $T_J - T_A$
1V	2.16W	20°C/W	68.2°C – 25°C

The thermal management of diode rectifiers are relatively easy compared to switching diode and MOSFET. The power loss of diode rectifiers is considerably low since passing current through them is low and the switching frequency of rectifier diodes is approximately between the range 20-40Hz due to low poles number of generator.

Another important heat generator are inductor and shunt resistance. The inductor can dissipate the heat from copper if ambient temperature is not high. Also, the operating temperature of inductors, motors and transformers are designed as 85°C. On the other hand, the shunt resistor is selected with consideration of resistive loss. Therefore, these components can stay cool sufficiently.

5.1. Thermal Simulation

The thermal managament of the semiconductors have great importance because short life-time, unreliability and low quality of safety of the device may cause undesirable situations. Therefore, the hand calculations having many assumptions and omission should be supported with thermal analysis.

The thermal thermal analysis has desinged in CAD program, Solidworks. The step file of the designed pcb has exported from KiCAD and imported to Solidworks, which provides thermal simulation with real and same size of the PCB. The thermal simulation can be made advanced with consideration flow analysis. However, the simulation is done with simulation tool solely.

The thermal analysis have inputs as seen in *Table 9*.

Table 9 Inputs of thermal simulation

Input	Componenets
Heat power of component	Mosfet
	Diode
	Inductor
	Shunt Resistance
Contact Sets	Case-to-leads
	Leads-to-board
Material types	PCB – FR4 (Thermal conductivity etc.)
	Semi-conductors
	Inductor and shunt resistance
Convection Coefficient	Natural air convection (2.5-25)
	Ambient temperature

Figure 19 shows the exploded PCB components to set contacts and to determine thermal resistances between materials. *Figure 20* shows the added contacts and PCB design in Solidworks.

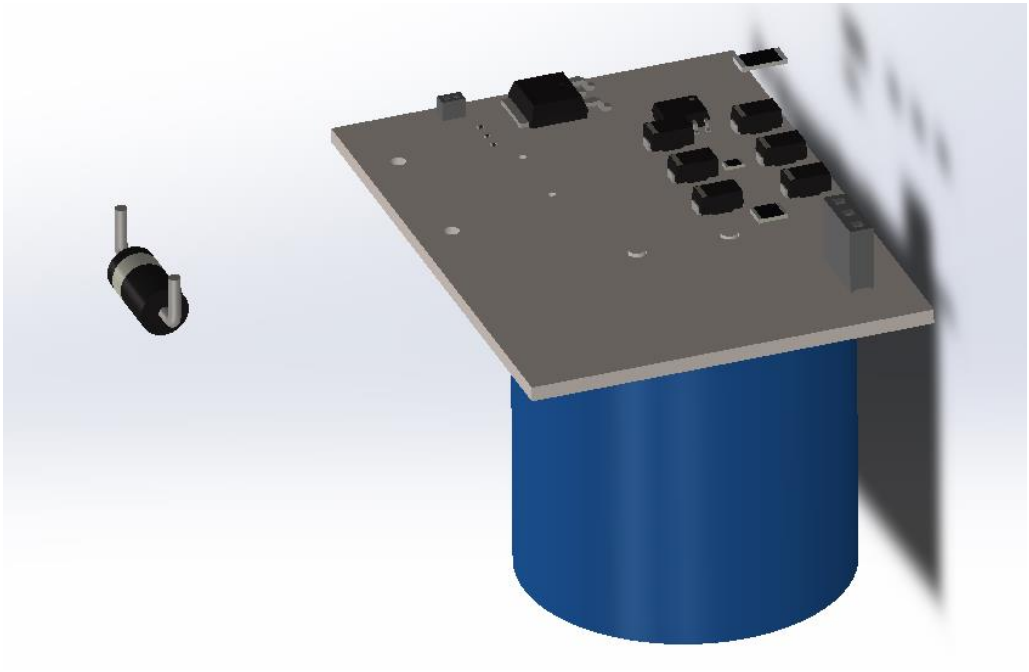

Figure 19 Exploded PCB design

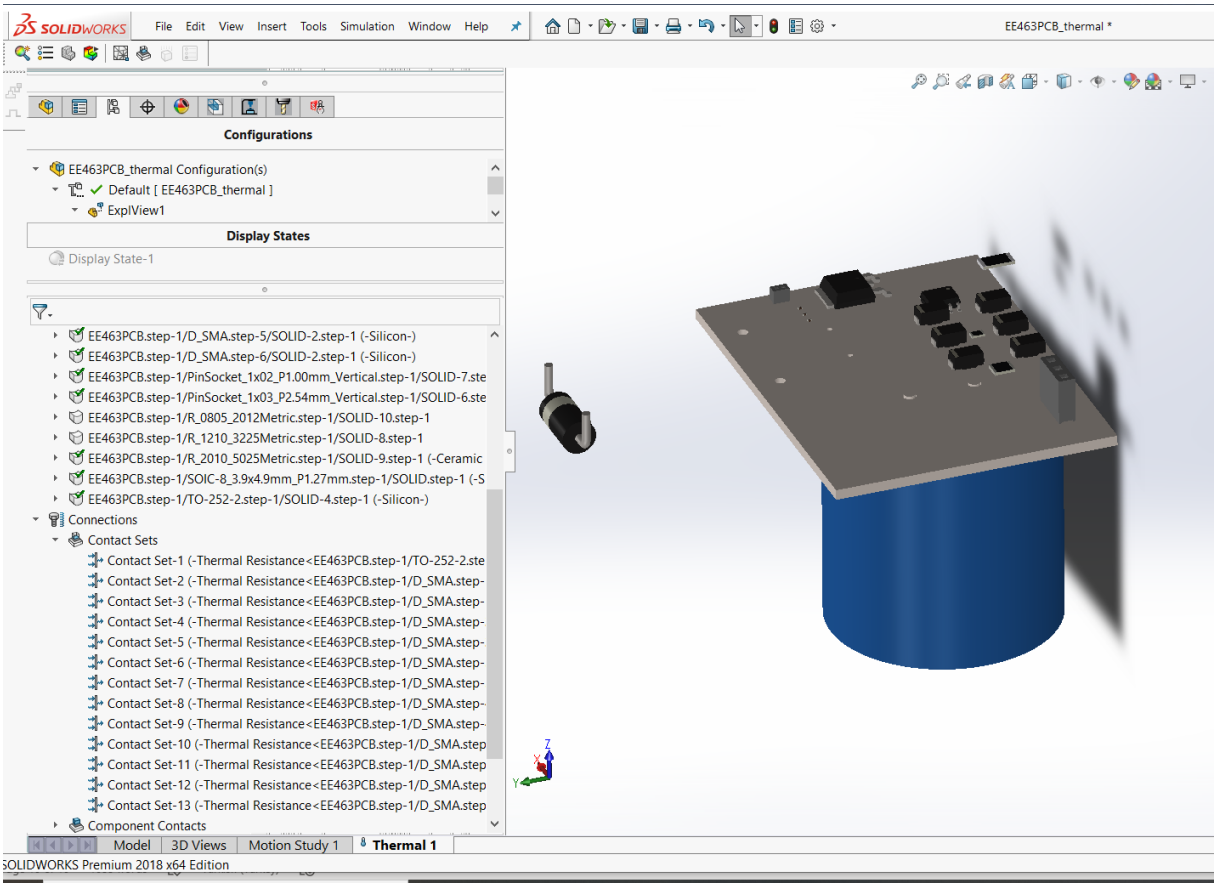

Figure 20 Added componenet contacts and thermal loads of the PCB design

6. Inductor Design

Ferrite Cores

Toroidal shape Ferrite core values have been examined as a starting point for designing the inductor for the buck converter with the specified rated values. One of the main properties of the ferrite cores is that their high permeability values, which increase flux density. Although it is quite easy to reach high inductor values with less winding, they have not been seen as a reasonable option in high current applications because of their low saturation flux density, which is generally around 0.5 T. According to the Formulas (5), since reducing the rated current is not an option and the radius value is limited by physical factors, the only option is to reduce the μ value to decrease operating flux density for allowing reasonable amount of N turns. Therefore, it has been considered appropriate to look at magnetic core materials with lower permeability and higher maximum flux density values. In case of ferrite core use, it has been decided to examine the changes in the case of including an air gap in the core design.

$$B = \frac{\mu N I}{2\pi r}, \qquad L = \frac{NBA}{I} \tag{5}$$

Iron Powder Cores

Iron powder toroidal cores have much lower permeability and higher saturation flux density values comparing with the toroidal ferrite cores. When the variables seen in the equation (…) are evaluated, the permeability decreases can only be caused by the increase in the number of turns. Even though keeping B value seems to be as desired due to the saturation effect, it makes that very difficult to reach the required level of inductance. Therefore, the problem with iron powder cores is requiring high number of turns. On the other hand, while inductance is proportional with the square of N (number of turns), flux density is proportional with N. Therefore, higher inductance values can be achieved with increasing N without effecting B field as much as the ferrite core case, due to the effect of low permeability.

Magnetic permeability has been decreased to achieve stable operation in the designed inductance. However, it also affects inductance proportionally, which can be observed from Equation …. For this reason, the highest possible permeability values of iron cores have been evaluated considering their optimum operating conditions. As can be examined in the Figure …., although type 26 material have higher permeability, it is suitable for DC applications. Therefore, type 3 material have been chosen as core material due to its high permeability and ability to operate at 0.05-0.5 MHz frequencies.

Iron Powder Magnetic Core Properties						
Mix	Color	Material	μ	Temp Stability (ppm/ °C)	f (MHz)	Uses
26	Yellow/White	Hydrogen Reduced	75	825	DC -1	EMI filters, DC chokes
3	Gray	Carbonyl HP	35	370	0.05 - 0.50	Exc. stability, good Q at low freq.
15	Red/White	Carbonyl GS6	25	190	0.10 - 2	Exc. stability, good Q
1	Blue	Carbonyl C	20	280	0.50 - 5	Exc. stability, good Q at low freq.
2	Red	Carbonyl E	10	95	2 -30	High Q
7	White	Carbonyl TH	9	30	3 - 35	Similar to mix 2 and mix 6, exc. temp stability
6	Yellow	Carbonyl SF	8	35	10 -50	Very good Q and temp. stability for 20-50 MHz
10	Black	Powdered Iron W	6	150	30 - 100	Good Q and stability for 40-100 MHz
12	Green/White	Synthetic Oxide	4	170	50 - 200	Good Q, moderate temp. stability
17	Blue/Yellow	Carbonyl	4	50	40 - 180	Similar to mix 12, better temp. stability, Q drops about 10% above 50 MHz, 20% above 100 MHz
0	Tan	Phenolic	1	0	100 - 300	L varies greatly with winding technique

Figure 21 Magnetic Core Properties

After the material selections, the required core size has been determined for the inductance value to be created. The A_L values of the different size of powder iron cores have been given in Figure 17, where A_L represents the how much μH does these core sizes supposed to have for 100 turns. The equations given in 17 can be used to calculate the required number of turns for a specific inductor value. According to the calculations considering A_l values given in Figure 17, T106 size of type 3 powder iron core have been selected with 182 turns.

$$N = 100 * \sqrt{\frac{L}{A_L}}, \qquad L = A_L * \left(\frac{N^2}{10^4}\right)$$

A_L Values											
	Mix Type										
Size	**26**	**3**	**15**	**1**	**2**	**7**	**6**	**10**	**12**	**17**	**0**
T-12	n/a	60	50	48	20	18	17	12	7.5	7.5	3.0
T-16	145	61	55	44	22	n/a	19	13	8.0	8.0	3.0
T-20	180	76	55	52	27	24	22	16	10	10	3.5
T-25	235	100	85	70	34	29	27	19	12	12	4.5
T-30	325	140	93	85	43	37	36	25	16	16	6.0
T-37	275	120	90	80	40	32	30	25	15	15	4.9
T-44	360	180	160	105	52	46	42	33	18.5	18.5	6.5
T-50	320	175	135	100	49	43	40	31	18	18	6.4
T-68	420	195	180	115	57	52	47	32	21	21	7.5
T-80	450	180	170	115	55	50	45	32	22	22	8.5
T-94	590	248	200	160	84	n/a	70	58	32	n/a	10.6
T-106	900	450	345	325	135	133	116	n/a	n/a	n/a	19
T-130	785	3350	250	200	110	103	96	n/a	n/a	n/a	15
T-157	870	420	360	320	140	n/a	115	n/a	n/a	n/a	n/a
T-184	1640	720	n/a	500	240	n/a	195	n/a	n/a	n/a	n/a
T-200	895	425	n/a	250	120	105	100	n/a	n/a	n/a	n/a

Figure 22 AL Values of Cores

After the size and type selections are made, it should be ensured that the selected core can operate without any saturation in flux density. The recommendation of the manufacturer company Amidon for the use of ferrite and iron powder materials is as follows:

"Saturation will decrease the permeability of the core causing it to have impaired performance or to become inoperative. The safe operation total flux density for most Ferrites is typically 2000 gauss, while the Iron Powders can tolerate up to 5000 gausses."

Flux density was found as 0.266 T in the calculation using equation 5. Considering this, it can be concluded that the designed inductor with the selected values is suitable for its intended use and will operate within the safe operation region.

Cable

The average and maximum current values passing through the inductor have been observed as 2 and 2.15 A respectively, Figure …. Therefore, the cable thickness to be used in the inductor windings have been chosen as 22 AWG (American Wire Gauge), which is able to carry 3A of current trough it at 60° with 0.644 mm thickness. Therefore, the main factor limiting the maximum current amount the inductor can carry is the thickness of the cable used. In the current design, the maximum current rating is set to 3A with 22 AWG cable thickness.

After finding the cable thickness, inductance value and the number of windings required to reach this inductance, it is time to calculate how much cable is spent for this number of windings. In this case, it has been found that a 7m 22 AWG coper cable is sufficient to wind 182 times around the selected core.

7. PCB Design

PCB Design

During PCB, the factors, which should be taken into consideration can be specified as follows:

- Radiated Electromagnetic Interference
- Conducted EMI
- Power Supply Stability
- Efficiency
- Operation Longevity
- The footprint of the components will be added to the design by looking at the datasheet. If that footprint is not already available in the program library used, the footprint will be created.
- Considering high voltage conditions, suitable trace spacing will be left according to IPC2221B standards.
- Space will be left for the heatsink, considering the components that consume high power.
- The appropriate track width will be calculated considering the IPC2221 standard. Magnitude of the current should be considered because high current causes heating in traces.
- Silk layer will be used as much as possible to make the design more descriptive.
- Copper thickness will be as recommended in the datasheet of the components used. For example, 1 oz / ft^2 is chosen for the rectifier.
- If necessary, control traces will be drawn on the inner layer to avoid noise.
- 90-degree angles will be avoided while drawing traces. Because this reduces the trace thickness, 45-degree angles should be used instead.
- If necessary, nodes will be made at important points.

Among these factors, EMI, electromagnetic disturbance, was considered as the most important factor that could cause PCB malfunction. Since one of the main reasons of Radiated Electromagnetic Interference is switching devices, special attention should be paid to the placement of the switching elements in the Buck Converter. Moreover, the loops of the switching elements should be as small as possible. For all these reasons, the input capacitor and inductor of the buck converter were the first circuit elements to be placed in the PCB design. A design was developed in which the inductor and capacitor loops were minimized as much as possible.

Circuit design is made on a double layer PCB. During the PCB design, 2 different options were considered while capacitor and inductor placements were performed. In the first of these options, all circuit elements are placed on the upper layer, while in the second option, the capacitor and inductor are placed on the lower layer. Since the first option causes the inductor and capacitor loops to lengthen, and therefore increasing the EMI effect on the PCB, the development has been continued with the second option. In addition to this, the circuit size has been reduced and the PCB price has been reduced with the two-sided PCB design, which can be observed in the Figure 19.

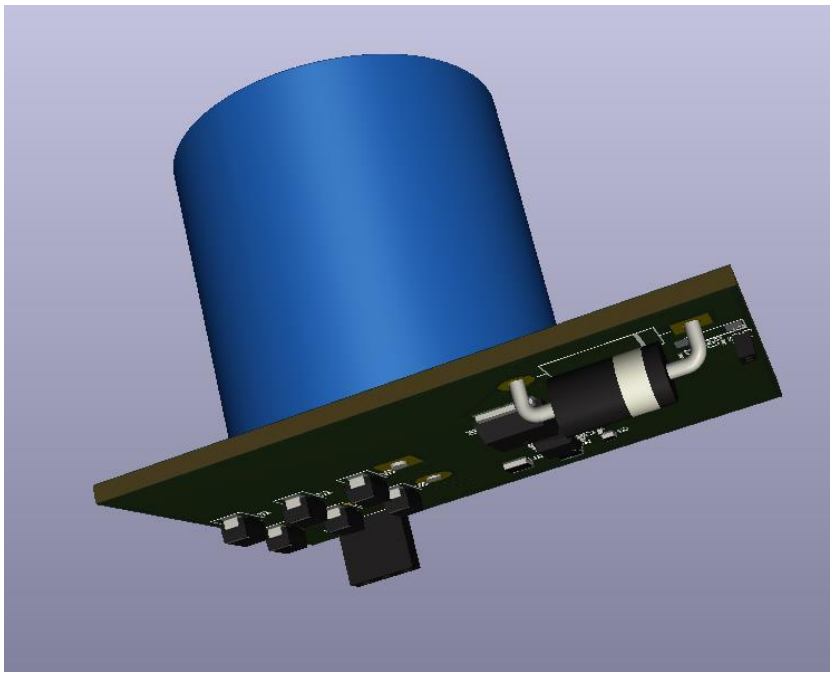

Figure 23: Two-sided PCB design view

Placement of the other circuit elements adjusted according to inductor and output capacitor of the rectifier. As can be observed in Figure 20, while MOSFET is placed near one of the inductor connections, output capacitors of the Buck Converter are placed near to its other connection. In addition, it has been deemed appropriate to keep the diode on the upper surface in order to leave the switching loop even smaller. Moreover, the controller IC is placed close to the MOSFET.

While the rectifier output capacitor is placed close to the rectifier outputs, it has been approximated to the converter circuit by taking physical limitations into account. The layout view of the PCB design can be observed from Figure 20, While red traces show connections on the upper layer, green traces show connections on the bottom layer of the PCB. In this layout, the circuit elements placed on the bottom surface are shown in pink colour.

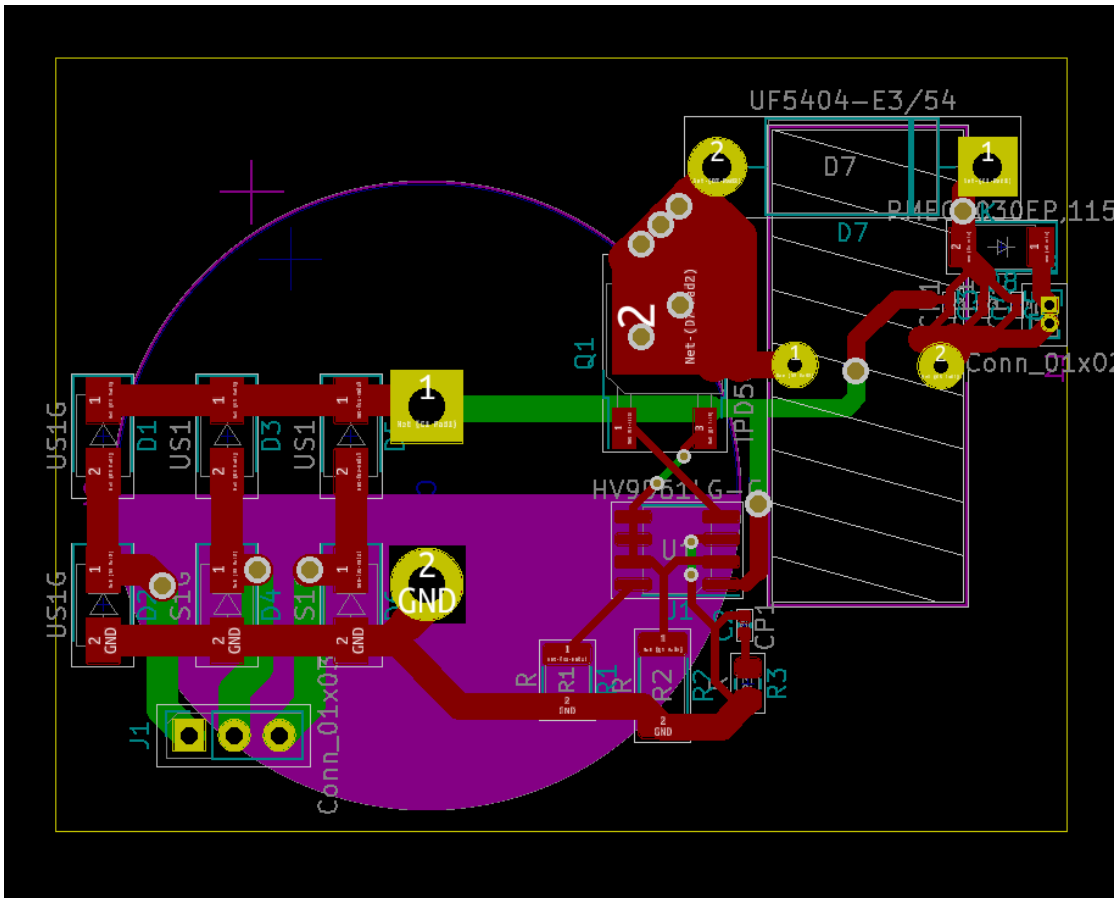

Figure 24: PCB design layout view without copper pouring

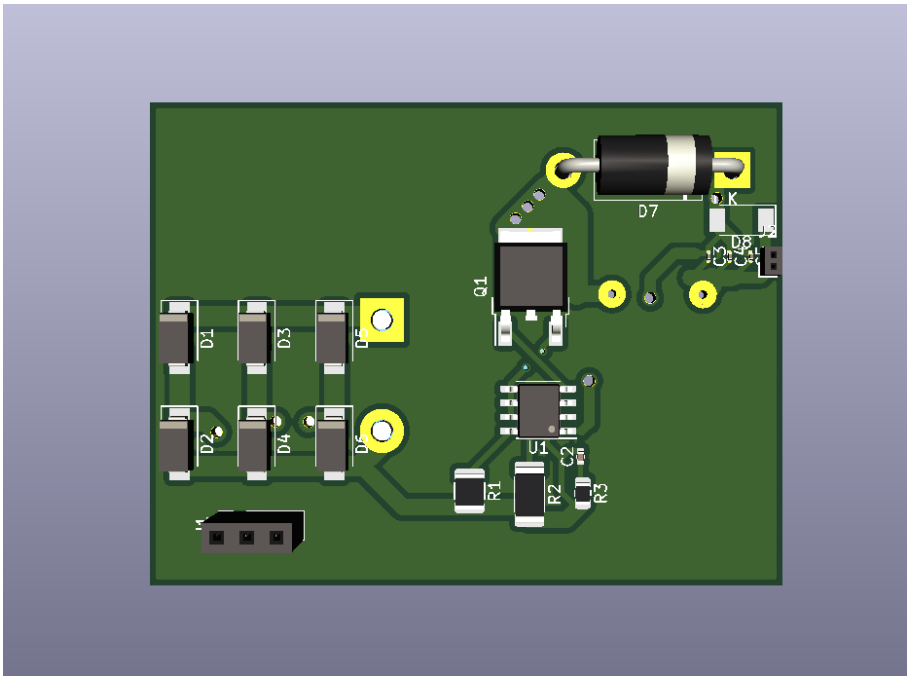

Figure 25: 3D top layer view of the PCB design

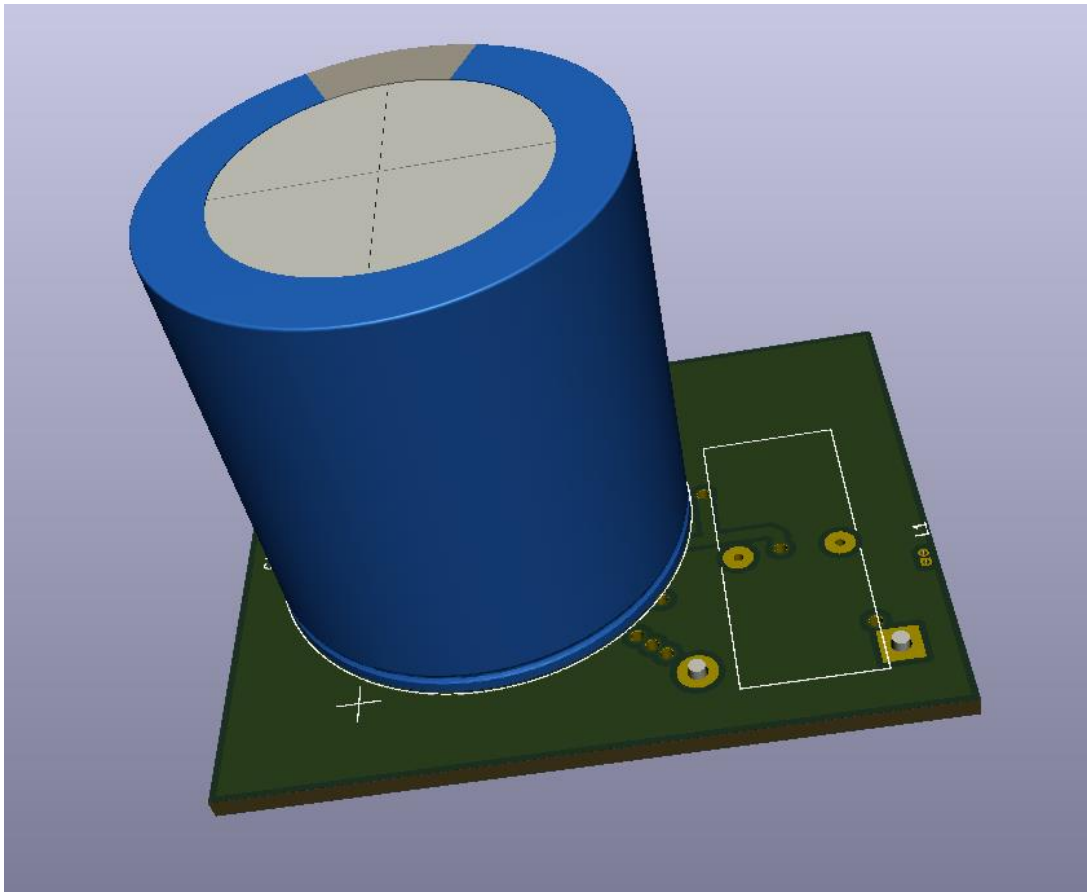

Figure 26: 3D bottom layer view of the PCB design

8. Component Selection

8.1. Component Selection for Buck Converter

Rectifier

In the market research on diodes, array diodes and three phase rectifiers were investigated. When the single diode cost and array diode cost were compared, it was understood that the surge current values of the array diodes were not sufficient in the cost range of six single diode. Also, voltage and current ratings of single phase and three phase array diodes was too large, therefore thermal calculation cannot be made without using heatsink in datasheets. Finally, the diode rectifier is constructed with single diodes. The separate usage has advantages in terms of cost and fault. The production of single diodes can be manufactured in huge amounts, which can provide them with low cost. Also, single diodes can be replaced easily. The important parameters are breakdown voltage and forward current ratings. There is no need to

fast diodes because the electrical frequency of generator cannot excess the 60Hz due to small pole-pair number.

Table 10 Rectifier component selection

Rectifier Diode	Reverse Voltage (V)	Forward Current(mean) (A)	Forward Current(peak) (A)	Forward Voltage (V)
S1G(Single)	400	1	10	1.1
3GBJ3516-BP (Three Phase)	1600	35	400	1.1
DLA5P800UC-TRL(Array)	800	5	70	1.18
Simulation	250	0.2	1.2	0.7

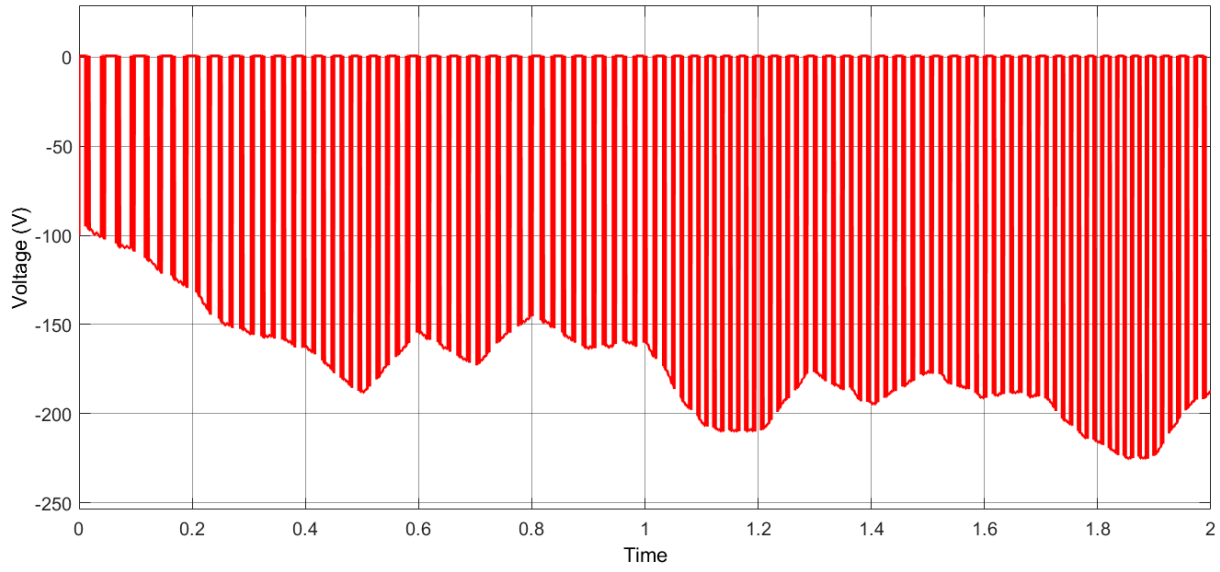

Figure 27 Voltage Waveform of Rectifier Diodes

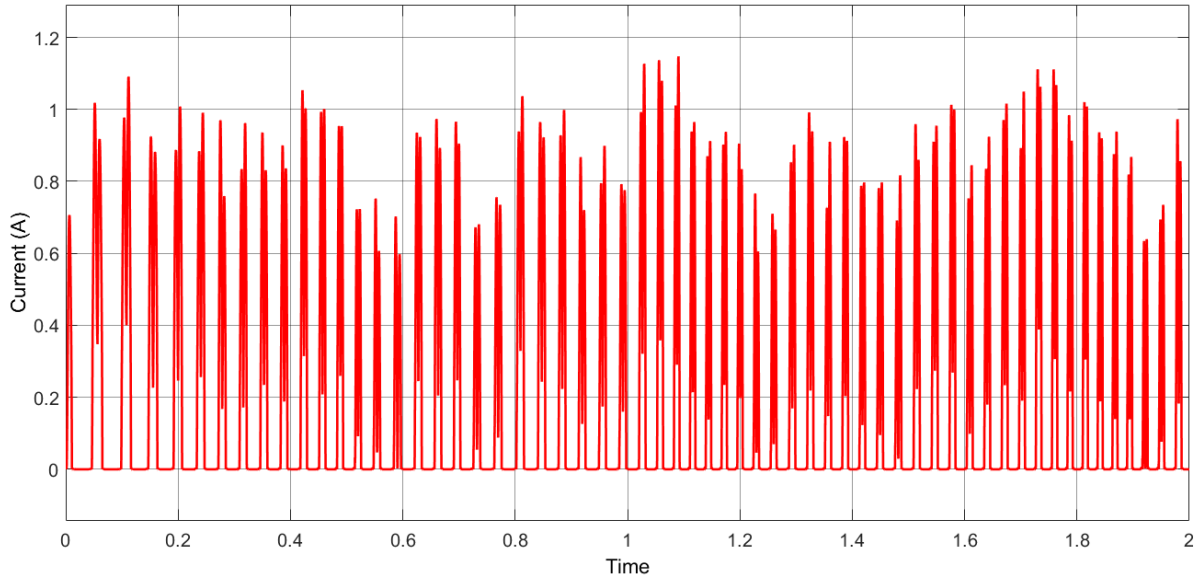

Figure 28 Current Waveform of Rectifier Diodes

DC Link Capacitor

Table 11 DC Link Capacitor component selection

Rectifier Capacitor	Capacitance (μF)	Voltage Rating (V)	Cost ($)	Height (mm)	Rated Ripple Current (mA)
MAL219856569E3-ND	56	400	3.91	27	720
450VXS390MEFC30X50	390	450	2.07(200 pieces)	52	2110
400HXG470MEFC30X50-ND	470	400	2.67(200 pieces)	52	3040
400USG470MEFC25X50	470	400	2.69 (200 pieces)	52	2390
380LX471M350A032	470	350	2.47(560 pieces)	37	2400

The 56 μF capacitor is sufficient for the design, so we chose the first capacitor in the Table 11 before. Subsequently, cheaper capacitors with higher capacitance are found in the market. When choosing capacitors, we paid attention to voltage ratings and current ripple values in steady state analysis of simulations. When we made a comparison in terms of price and size, we decided to choose the capacitor at the bottom of the Table 11.

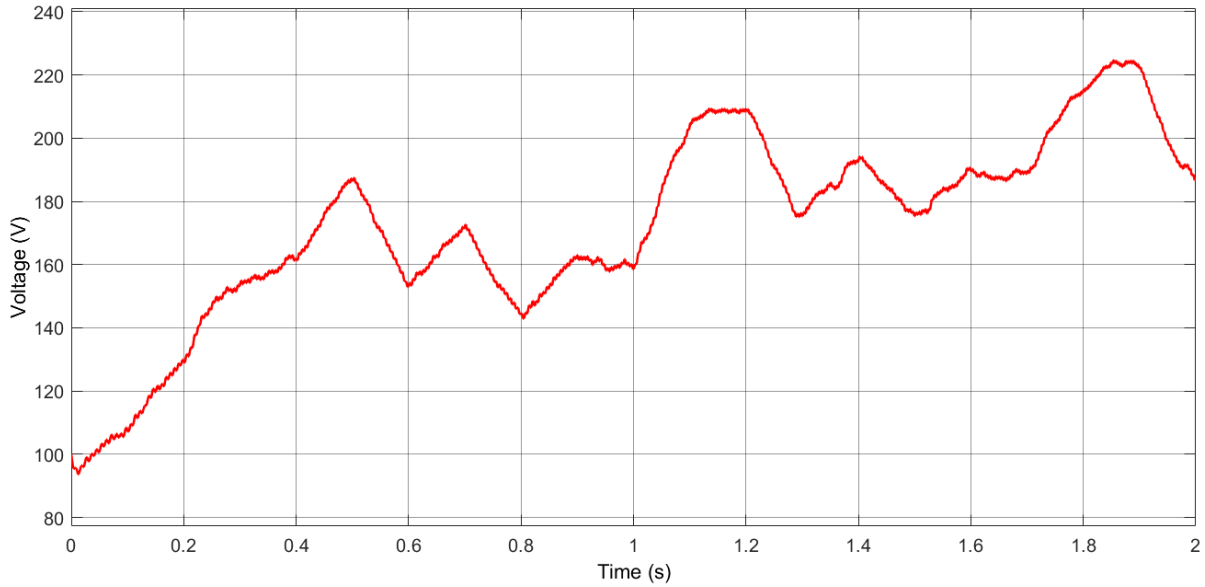

Figure 29 Voltage Waveform of DC Link Capacitor

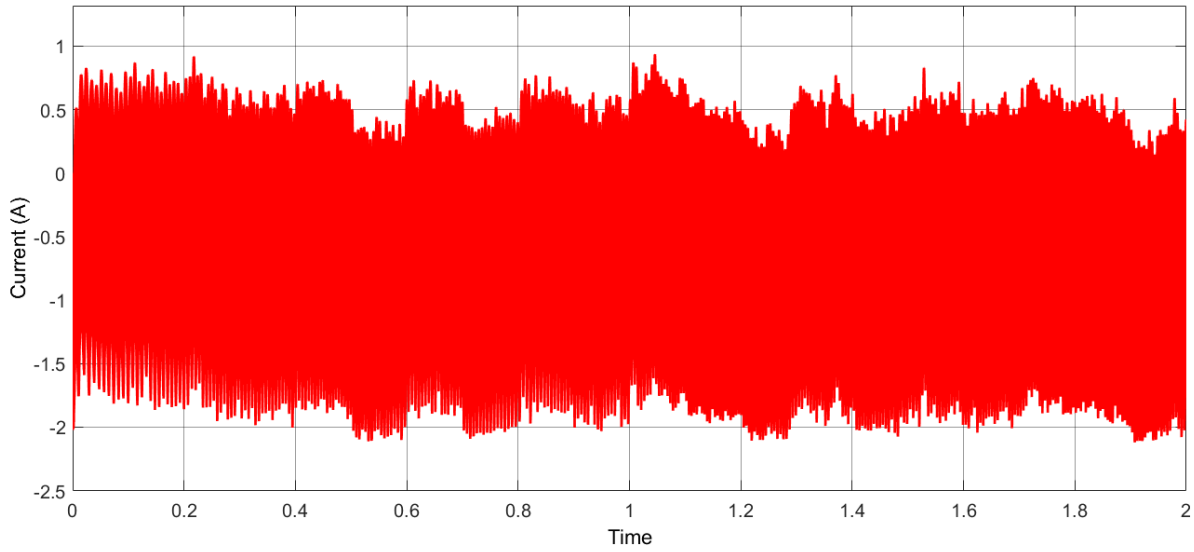

Figure 30 Current Waveform of Rectifier Diodes

Inductor

Table 12 Inductor component selection

	Inductance (mH)	Current Rating (A)	Saturation Current	Price ($)
1140-272K-RC	2.7	2.2	3.9	9.56
AIRD-03-152K	1.5	2	3.4	5.52
PowerGuide Inductor	1.5	3	4.06	3.23 $

The main point while choosing an inductor is its current ratings in addition to inductance. Even though, 2A average values expected on top of the inductor, it was observed in that the current value on the inductor can reach peak values of 2.15 A. Therefore, special attention has been given to the saturation currents during the selection of the inductor. The inductor models which use ferrite core as magnetic material have been preferred due to their ability to operate at higher frequencies and allowing higher inductor values with smaller size. Two different inductor values have been compared to determine the advantages and disadvantages each have. Even though, high inductance value can decrease the output current ripple even further, considering the price of 1140-272K-RC, choosing AIRD-03-152K evaluated to be more appropriate. When the %10 tolerance of the AIRD-03-152K also included, it can be said that this inductor will not cause any problem in providing the required inductance value for the converter to supply current within the previously specified ripple current range. After making these comparisons, we decided to design an inductor for making cheaper and learning purposes, and we used our own inductor in the project.

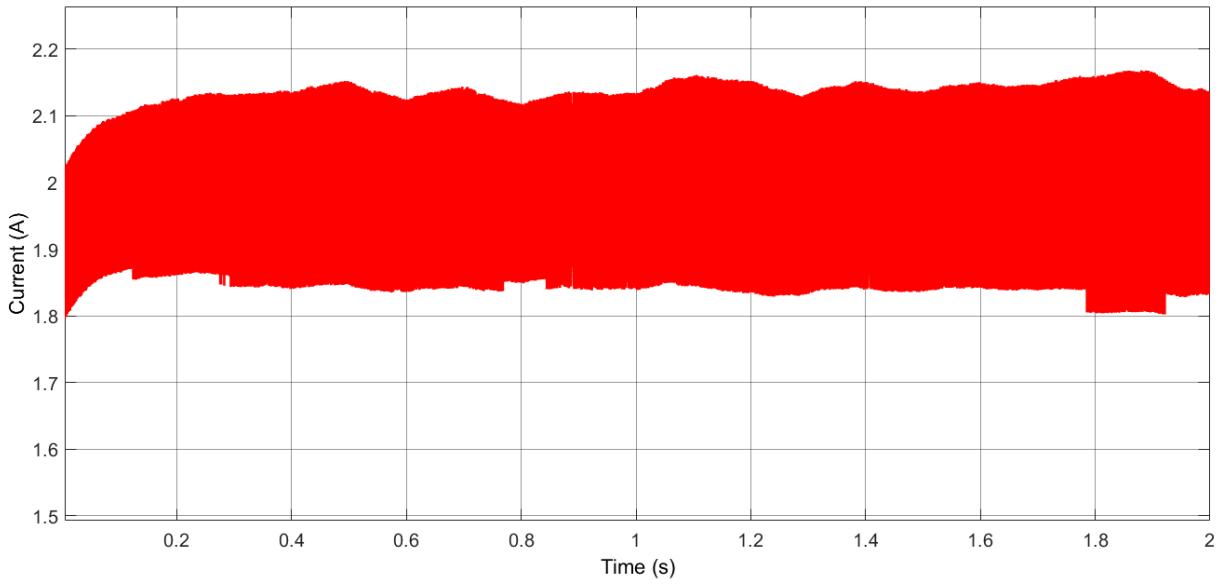

Figure 31 Current Waveform of Inductor

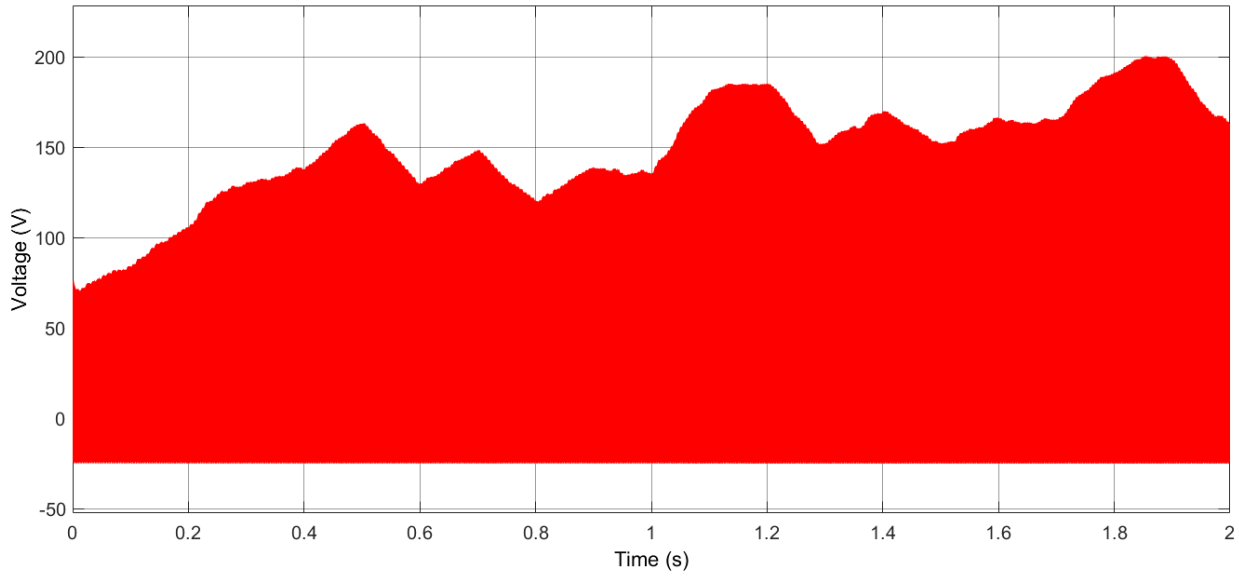

Figure 32 Voltage Waveform of Inductor

Capacitor

Capacitor selection process was carried out according to Equation 5. In the first step, aluminium electrolytic capacitors were evaluated with a 68 µH capacitance and 0.220 Ω ESR values. As can be seen from Figure 33, this capacitance value was not sufficient for the ESR value where the selected capacitor has. Therefore, the ESR values of different capacitor types were compared with the decision to use a different capacitor. During these comparisons, it was observed that the ESR values of ceramic capacitors were less than 0.015 Ω. In this case, it was decided to connect 3 ceramic capacitors in the same size in parallel to provide reduction in both ESR and capacitance values. As a result of all these evaluations, it was deemed appropriate to use 3 capacitors of 4.7 µF. Considering the new capacitor selection, there was an improvement of %600 in capacitance, %4400 in ESR, and 0.1 $ improvement in price. In addition, small size of the ceramic capacitors, and the selection of SMD type have reduced the space spent on output capacitor of Buck Converter drastically.

$$C_o = \frac{1}{8 * f_{sw} * (\frac{\Delta V}{\Delta I_L} - ESR)} \quad (4)$$

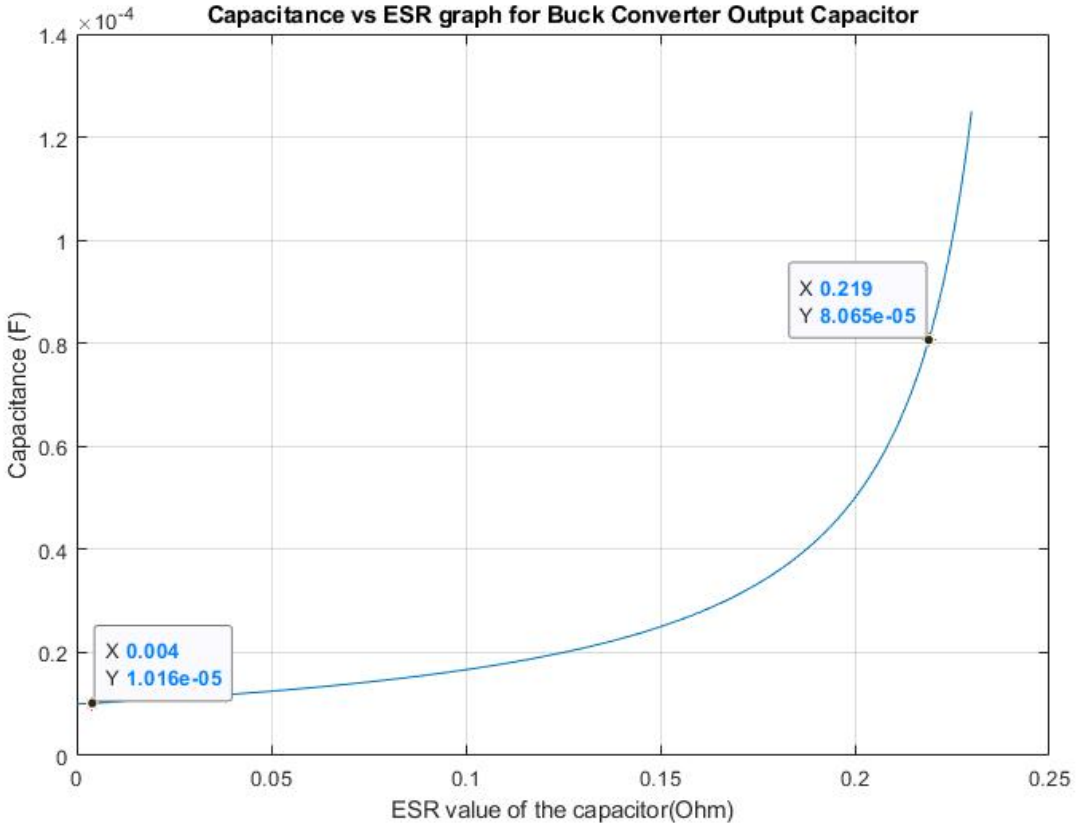

Figure 33 Capacitance vs ESR graph - Buck converter, Output Capacitor

Table 13 Capacitor component selection

Buck Converter Capacitor	Capacitance (µF)	Voltage Rating (V)	Cost ($)	Size (mm)	ESR (mΩ)
ESC686M035AE3AA	68	35	3*0.07232	22 (diameter)	220
GRM188R6YA475KE15D	4.7	35	0.11537	1.6 (length)	100

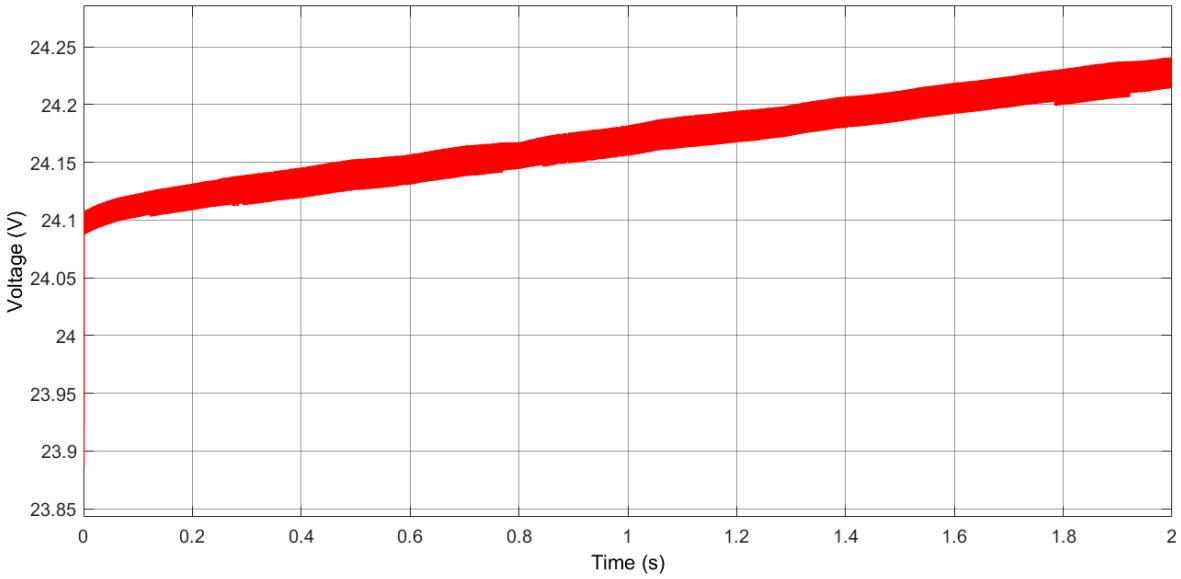

Figure 34 Voltage Waveform of Converter Capacitor

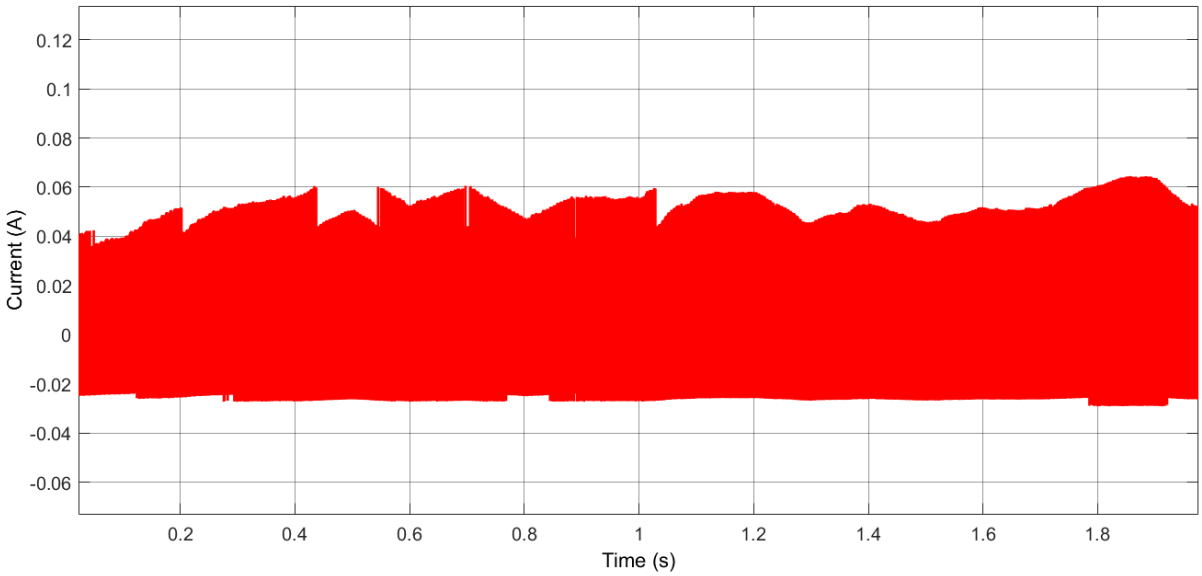

Figure 35 Current Waveform of Converter Capacitor

Diode

As the diode will guide the converter during the OFF times of the MOSFET, which will be about %90 due to the input and output voltage rate of the rectifier, it chose to be super-fast rectifier diode, which lowers the switching losses due to its fast reverse recovery time. While choosing diode, it should be also considered that the voltage rating across it will be approximately around 400 V coming from the rectifier voltage.

Table 14 Diode component selection

Diode (Buck Conv)	V_{RRM} (V)	$I_{F(AV)}$ (A)	V_{FD} (V)	Q_{rr} (nC)	Cost $
ES3G	400	3	1.1	50	0.18
UF5404 E3/54	400	3	1.0	8	0.224

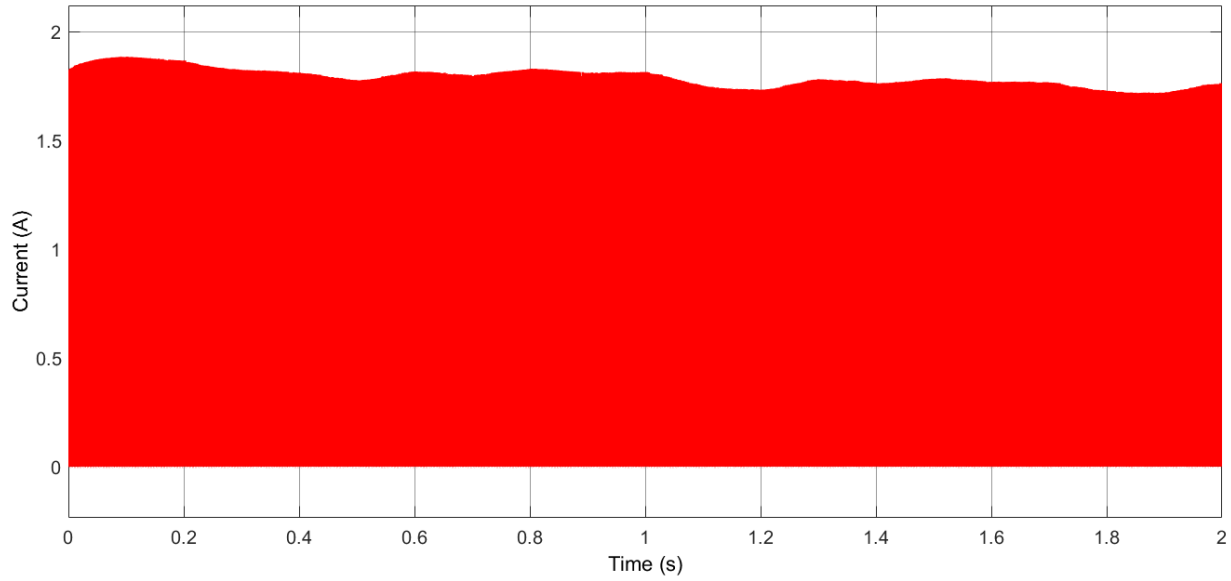

Figure 36 Current Waveform of Freewheeling Diodes

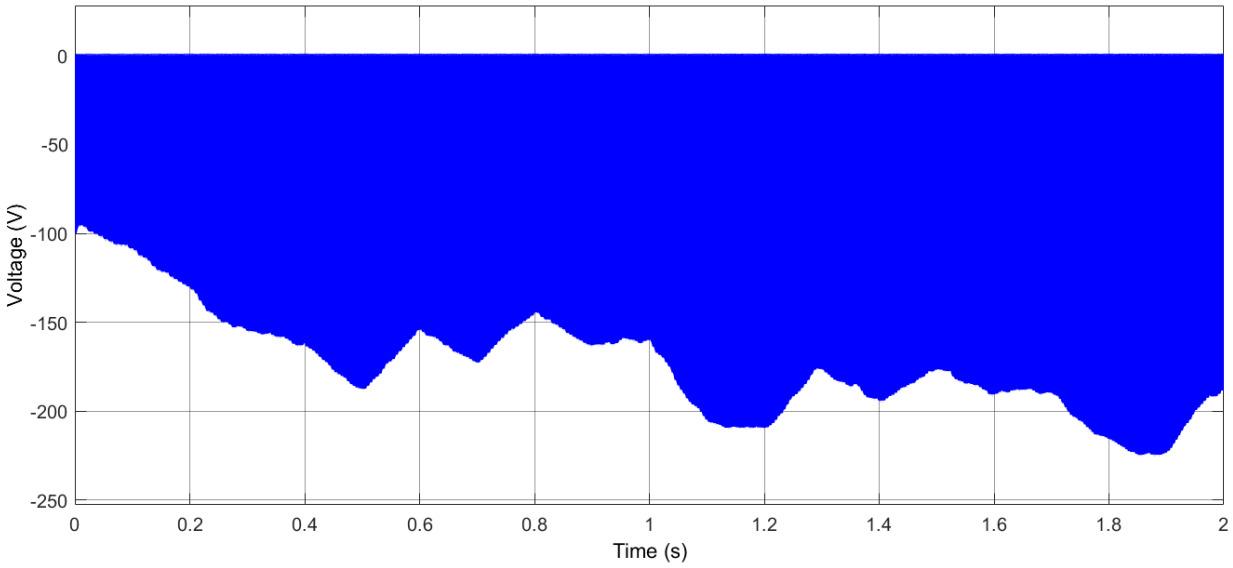

Figure 37 Voltage Waveform of Freewheeling Diodes

MOSFET

The most important parameter while choosing a MOSFET for switching applications is its Ron resistance to decrease conduction loss. Different type of MOSFTET have been compared and IPD50R650CEAUMA1 have been found to be more suitable to use in the converter, considering its resistance and price.

Table 15 MOSFET component selection

	V_{DS} (V)	$R_{DS\,(on)}$ (Ω)	I_D (A)	Price($)
SPN04N60S5	600	0.95	0.8	Non-stock
IPU60R1K4C6	650	1.4	3.2	0.33
IPS60R1K0PFD7S	650	1.0	4.7	0.31
IPD50R650CEAUMA1	500	0.65	9	0.31

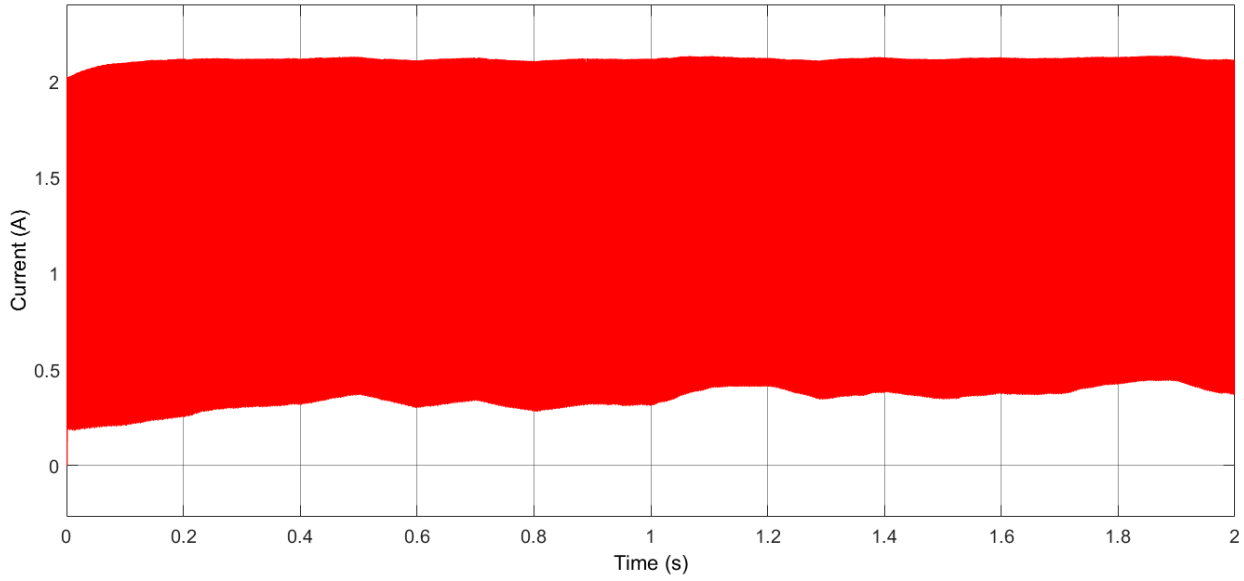

Figure 38 Current Waveform of MOSFET

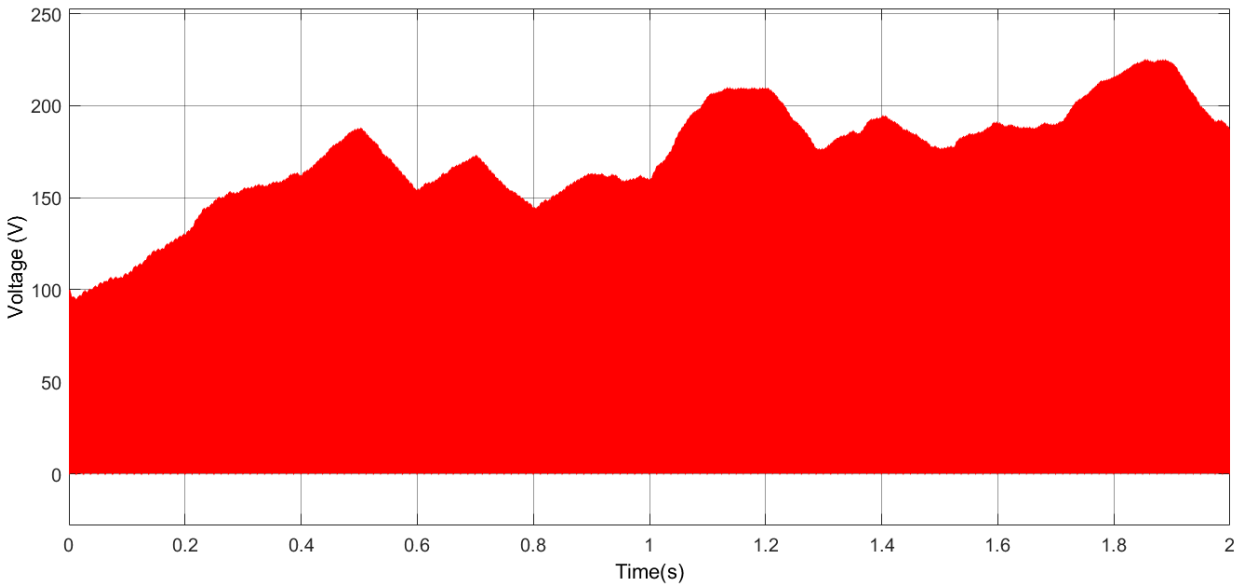

Figure 39 Voltage Waveform of MOSFET

Controller

Table 16 Controller component selection

Controller	V_{IN} (V)	Min on Time (ns)	Cost
HV9961LG-G	8-450	430	1.19$

In market research about controller, we could not find the controllers containing its MOSFET with an input voltage above 150 V, so we decided to buy this controller whose MOSFET is connected externally. Thanks to this controller, gate driver is not needed.

Controller Resistors

Table 17 Controller Resistors selection

Resistors	Resistance (Ω)	Power (W)	Tolerance (%)
VDD Resistor RK73B2ATTD204G	200 k	0.25	2
Frequency Resistor RK73H2ETTD4023F	402 k	0.5	1
Current Sense Resistor CSRN2010JKR130	0.13	1	5

Required resistance are calculated datasheets of the controller, and resistors are chosen by taking into consideration rated power values. Shunt resistor is selected from current sense resistors.

Controller Capacitor

Table 18 Controller Capacitor selection

VDD Capacitor	Capacitance (µF)	Voltage Rating (V)	Cost ($)	Size (mm)
C2012X7R1C225K125AB	2.2	16	0.045	2*1.25

SMD capacitors are investigated for the controller parts because SMD capacitors size is lower than THT capacitors.

Battery Diode

Table 19 Battery component selection

Battery Diode	V_{RRM}	$I_{F(AV)}$	V_{FD}	Q_{rr}	Cost
PMEG3030EP,115	30V	3A	0.36	0	0.12$

For this part of the topology, Schottky diode is chosen because Schottky diodes have low forward voltages and their losses mostly are due to reverse leakage currents. The diode will be in on mode in normal conditions; therefore, losses will be less with respect to other types of diode.

Inductor Selection and Calculations

Ferrite Cores

Toroidal shape Ferrite core values have been examined as a starting point for designing the inductor for the buck converter with the specified rated values. One of the main properties of the ferrite cores is that their high permeability values, which increase flux density. Although it is quite easy to reach high inductor values with less winding, they have not seen as a reasonable option in high current applications because of their low saturation flux density, which is generally around 0.5 T. According to the Equation (9), since reducing the rated current is not an option and the radius value is limited by physical factors, the only option is to reduce the µ value to decrease operating flux density for allowing reasonable amount of N turns. Therefore, it has been considered appropriate to look at magnetic core materials with lower permeability and higher maximum flux density values. In case of ferrite core use, it has been decided to examine the changes in the case of including an air gap in the core design.

$$B = \frac{\mu N I}{2\pi r}, \qquad L = \frac{NBA}{I} \tag{9}$$

Iron Powder Cores

Iron powder toroidal cores have much lower permeability and higher saturation flux density values comparing with the toroidal ferrite cores. When the variables seen in the Equation (9) are evaluated, the

permeability decreases can only be caused by the increase in the number of turns. Even though keeping B value seems to be as desired due to the saturation effect, it makes that very difficult to reach the required level of inductance. Therefore, the problem with iron powder cores is requiring high number of turns.

Cable

The average and maximum current values passing through the inductor have been observed as 2 and 2.15, in **Error! Reference source not found.**. Therefore, the cable thickness to be used in the inductor windings have been chosen as 22 AWG (American Wire Gauge), which is able to carry 3A of current trough it at 60° with 0.644 mm thickness.

9. Bills of Materials

While we were choosing components, we made sure that each product had at least 1000 sales in order to be included in the cheapest design bonus. Rectifier Capacitor is sold in packages of 560. In addition, the controller is sold in packages of 100. Unfortunately, there is no cheaper alternative sold in 1000 packages. Unfortunately, we could not find a cheaper one with more sales. Also, Buck Converter Diode is sold in packages of 500 and 1400. When calculating, 1400 packages are taken into consideration. If the package of 500 is taken into account, the unit price is $ 0.29286, and the cost will be $ 0.05482 more. Since we designed the Inductor, we purchased 1000 Toroid and it is enough to buy 23 packages of cables for 1000 inductors. Also, we have not included the cost of shipping charges when calculating cost of PCB, if PBCs are able to be ordered by FedEx for Turkey and its cost is $ 98. In this case, the unit price will increase by $ 0.098. In the design, extra diode is added to topology as an extra feature so that there is no energy loss from the battery when the wind turbine is not rotating and there is no reverse load on the system. If battery diode is not used, the unit cost should decrease by $ 0.12193.

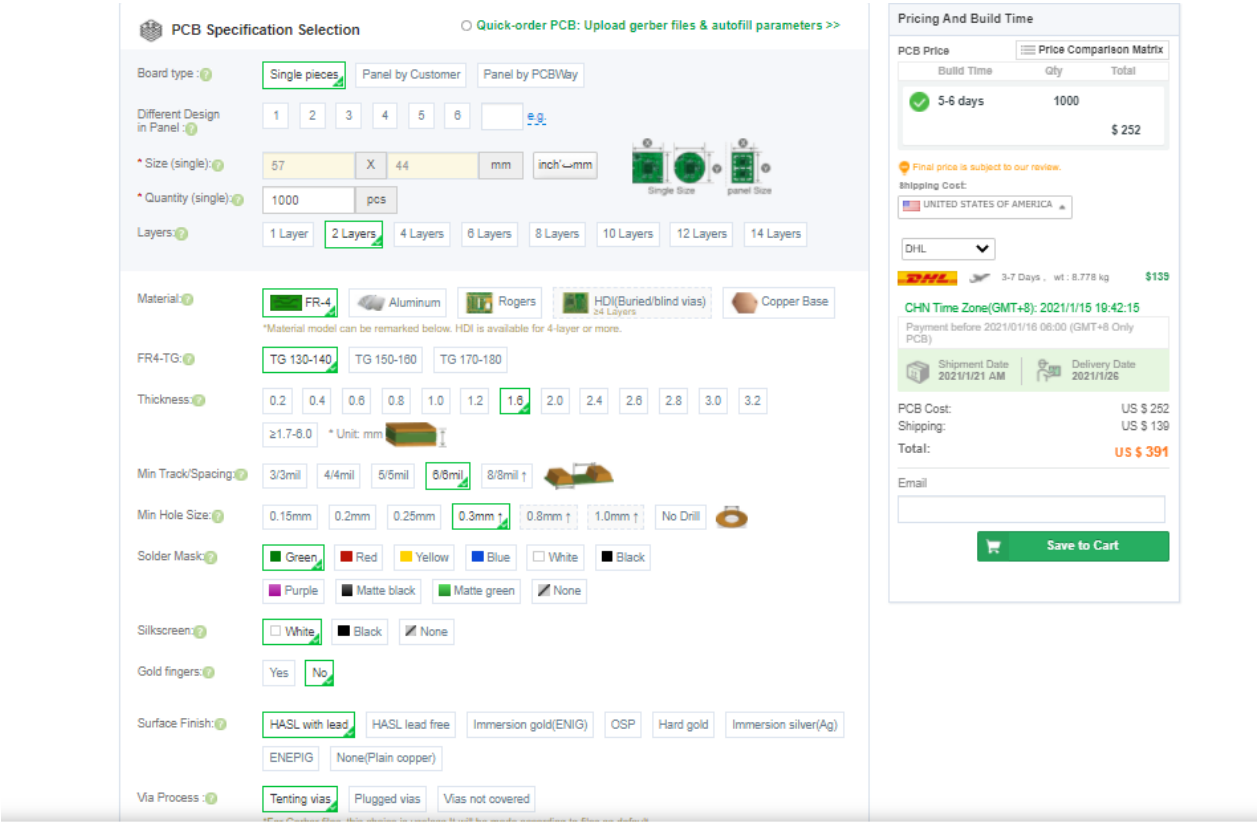

Figure 40 PCB Cost Calculations

10. Industrial Design

After the PCB design was completed, the industrial box where the design can be placed was determined by considering the values such as PCB width and component lengths etc. Considering these values, the main factor determining the length of the design was observed as the capacitor length, which is 37 mm long. In additionally, PCB width and length measured as 57 and 43.5 mm. According to these values, the 46x59x51 mm aluminum box shown in Figure 41 has been deemed appropriate for the circuit design. Therefore, the total system is expected to occupy a volume of 138.414 cm^3.

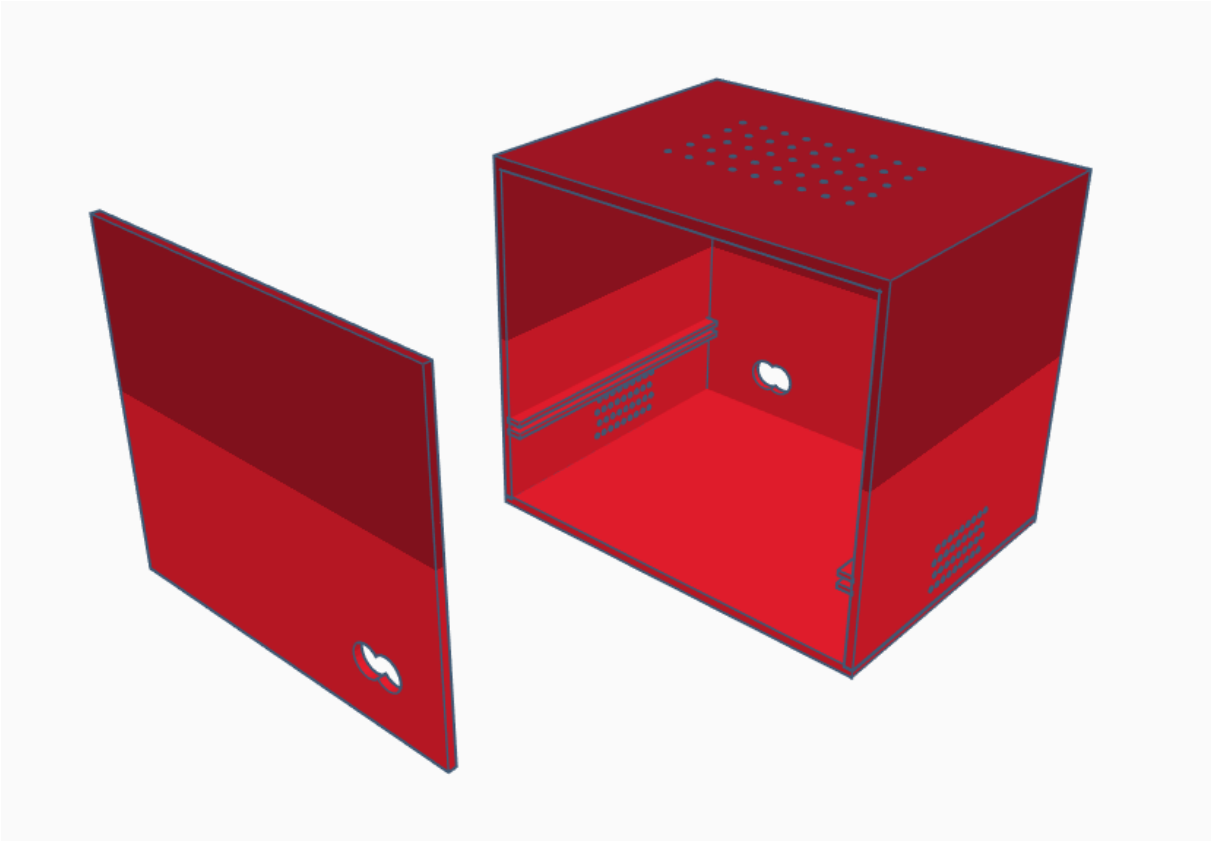

Figure 41 Aluminum box design for the system

Table 20 Bill of Materials

Index	Component Name	**Part Number**	**Manufacturer Part Number**	**Description**	**Package Quantity**	**Unit Price**	**Unit Cost**
1	Rectifier Diode	S1GFSCT-ND	S1G	DIODE GEN PURP 400V 1A SMA	1000	0.04284	0.25704
2	DC-Link Capacitor	380LX471M350A032-ND	380LX471M350A032	CAP ALUM 470UF 20% 350V SNAP	560	2.46961	2.46961
3	Buck Converter Diode	UF5404-E3/54GITR-ND	UF5404-E3/54	DIODE GEN PURP 400V 3A DO201AD	1400	0.22456	0.22456
4	Inductor Core	T106-3 Micro metals Iron Powder Toroid		Used for high Q applications below 1MHz.	1000	1.5	1.5
5	Inductor Cable	2328-22BCW1000-ND	22BCW1000	WIRE BUS BAR 22AWG 1000	23	1.73236	1.73236
6	Buck Converter Capacitor	490-7205-1-ND	GRM188R6YA475KE15D	CAP CER 4.7UF 35V X5R 0603	1000	0.11537	0.34611
7	Buck Converter MOSFET	448-IPD50R650CEAUMA1CT-ND	IPD50R650CEAUMA1	CONSUMER	1000	0.31024	0.31024
8	Controller	HV9961LG-GCT-ND	HV9961LG-G	IC LED DRIVER CTRLR DIM 8SOIC	100	1.19	1.19
9	Controller Resistor 1	2019-RK73B2ATTD204GCT-ND	RK73B2ATTD204G	RES 200K OHM 2% 1/4W 0805	1000	0.01179	0.01179
10	Controller Resistor 2	2019-RK73H2ETTD4023FCT-ND	RK73H2ETTD4023F	RES 402K OHM 1% 1/2W 1210	1000	0.02671	0.02671
11	Controller Resistor 3	CSRN2010JKR130-ND	CSRN2010JKR130	RES 0.13 OHM 5% 1W 2010	1000	0.084	0.084
12	Controller Capacitor	445-1420-1-ND	C2012X7R1C225K125AB	CAP CER 2.2UF 16V X7R 0805	1000	0.04554	0.04554
13	Battery Diode	1727-5324-1-ND	PMEG3030EP,115	DIODE SCHOTTKY 30V 3A CFP5	1000	0.12193	0.12193
14	PCB			2 LAYER 57*44 mm^2	1000	0.252	0.252
						Total Cost	8.57189

11. Conclusion

Within the scope of this project, it is ensured that the irregular energy coming from the wind turbine is stabilized with the help of rectifier and converter, and the battery is fed with a regular current. Moreover, duty cycle control of the MOSFET gate was carried out with the work done on the buck converter controller. In addition, during the component selection, converter operating frequencies, voltage and current values of the circuit elements that must operate continuously were taken into consideration. Finally, the dimensions and temperature values of the circuit were calculated with PCB design and thermal analysis.